University of Central Florida

STARS

2022

A Novel Antibody-Dependent MC-LR Detecting Biosensor for Early Warning of Harmful Algal Blooms (HABs)

Stephanie Stoll
University of Central Florida

A NOVEL ANTIBODY-DEPENDENT MC-LR DETECTING BIOSENSOR FOR
EARLY WARNING OF HARMFUL ALGAL BLOOMS (HABs)

by

STEPHANIE STOLL
B.S. University of Central Florida, 2020

A thesis submitted in partial fulfillment of the requirements
for the degree of Master of Science
in the Department of Civil, Environmental, and Construction Engineering
in the College of Engineering and Computer Science
at the University of Central Florida
Orlando, Florida

Summer Term
2022

Major Professor: Woo Hyoung Lee

ABSTRACT

Microcystins (MCs) are toxins produced by cyanobacteria commonly found in harmful algal blooms (HAB) occurring in many surface waters. Due to their toxicity to humans and other organisms, the World Health Organization (WHO) set a guideline of 1 μg L^{-1} for microcystin-leucine-arginine (MC-LR) in drinking water. However, current analytical techniques for the detection of MC-LR such as liquid chromatography-mass spectrometry (LC-MS) and enzyme-linked immunosorbent assay (ELISA) are costly, bulky, time-consuming, and mostly conducted in a laboratory, requiring highly trained personnel. Therefore, an analytical method that can be used in the field for rapid determination is essential. In this study, an Anti-MC-LR/MC-LR/Cysteamine coated screen-printed carbon electrode (SPCE) biosensor was newly developed to detect MC-LR, bioelectrochemically, in water. The functionalization of the electrode surface was examined using scanning electron microscopy-energy dispersive X-Ray spectroscopy (SEM-EDX) and X-Ray photoelectron spectroscopy (XPS). The sensor performance was evaluated by electrochemical impedance spectroscopy (EIS), obtaining a linear working range of MC-LR concentrations between 0.1 and 100 μg L^{-1} with a limit of detection (LOD) of 0.69 ng L^{-1}. Natural water samples experiencing HABs were then collected and analyzed using the developed biosensor and validated using ELISA, demonstrating the excellent performance of the biosensor with a relative standard deviation (RSD) of 0.65%. The interference and selectivity tests showed a minimal error and RSD values against other common MCs and possible coexisting ions found in water, suggesting high selectivity and low sensitivity of the biosensor. The biosensor showed acceptable functionality with a shelf life of up to 12 weeks. Overall, the Anti-MC-LR/MC-LR/Cysteamine/SPCE biosensors can be an innovative solution with characteristics that allow for

in situ, low-cost, and easy-to-use capabilities which are essential for developing an overarching and integrated "smart" environmental management system.

Keywords: Antibody, Cyanobacteria, Electrochemical biosensor, Harmful algal blooms (HABs), MC-LR, Microcystin toxins

ACKNOWLEDGMENTS

I would like to acknowledge and express my deepest gratitude to my advisor, Dr. Woo Hyoung Lee for his sincere support, excellent guidance, and prompt feedback. I am extremely grateful to him for giving me the opportunity to grow professionally and academically in his research lab. Without his support and encouragement, I would have not achieved what I did during my graduate career. I would also like to thank my committee members Dr. Andrew Randall and Dr. Anwar Sadmani for all the time and effort spent in the development of this thesis.

I would like to thank my friends and colleagues Dr. Jaehoon Hwang and Mohsen Pilevar for all their knowledge, assistance, and friendship, which helped guide me through my graduate career. I would also like to express my deep gratitude to Melissa Saint James for her patience and disposition to help. To all of you, thank you, this would have been much more difficult without you.

Finally, I express my thanks to my family and friends for their support and endless encouragement.

TABLE OF CONTENTS

LIST OF FIGURES

LIST OF TABLES

LIST OF ACRONYMS

CV – Cyclic voltammetry

CyanoHABs – Cyanobacterial harmful algal blooms

EIS - Electrochemical impedance spectroscopy

ELISA - Enzyme-linked immunosorbent assay

GCE – Glassy carbon electrode

MC – Microcystin

MC-LR – Microcystin-leucine arginine

NP – Nanoparticle

PB – Phosphate buffer

PBS – Phosphate buffer saline

SAM – Self assembled monolayer

SPCE – Screen printed carbon electrode

SPGE – Screen printed gold electrode

CHAPTER 1: INTRODUCTION

1.1. Introduction

Freshwater and estuarine ecosystems that provide critical habitats for diverse species of flora and fauna while supporting recreational activities and tourism businesses are frequently threatened by the increasing occurrences of cyanobacterial harmful algal blooms (cyanoHABs). While cyanoHABs disrupt the balance of various life forms in aquatic ecosystems, cyanotoxins produced by cyanobacteria can endanger human and aquatic organisms at all taxonomy levels [1]. Airborne and waterborne cyanotoxins may cause serious health problems for local residents as well as economic losses throughout multiple segments of the society [2]. Microcystins (MCs), also known as hepatotoxins, are the most common cyanotoxins associated with freshwater cyanoHABs. Human exposure to MCs can cause acute or chronic health hazards [3]. Many studies have found that liver is the main target organ of microcystin toxins, resulting in liver or even colon cancer. Other studies reported noticing kidney, reproductive, and developmental issues after exposure to the toxin. Additional research found that exposure to the cyanobacteria cell itself can also be harmful, resulting in gastrointestinal (GI) inflammation as well as dermatologic, eye/ear, and respiratory irritation [4].

There are currently over 240 known MCs, of which the most common and toxic is microcystin-leucine-arginine (MC-LR) with a tolerable daily intake (TDI) of 0.04 $\mu g\ kg^{-1}$ body weight per day [5]. The majority of States in the United States (US) and other countries have their own set of guidelines for these toxins [6]. The World Health Organization (WHO) set a guideline of 1 $\mu g\ L^{-1}$ for MC-LR in drinking water and the US Environmental Protection Agency (EPA) recommends a recreational value of 8 $\mu g\ L^{-1}$ [7]. The livability of a community around the HAB

affected waterbodies can deteriorate due to health risks and reduced aesthetic appeal of the surrounding environment.

CyanoHABs occur in many surface waters and hence, the occurrence, extent, duration, intensity, and timing of HAB events are critical to local communities, businesses, and policymakers. Florida's waterbodies, for instance, experience severe HABs due to increased eutrophication and warm temperatures, causing immense damage to the aquatic life and threatening residents' well-being and the local tourism-based economy. It is important to monitor the occurrence of HABs and the concentrations of cyanotoxins which are being produced by cyanobacteria to warn people in the area to stay away if the level of MC-LR concentration becomes too high. There exist visual observation [8], hyperspectral images (HSI) sensor [9], and satellite image-based tools [10] for monitoring cyanoHABs. However, cyanotoxin production is highly variable regardless of the presence of cyanobacteria and toxins can occur at unsafe levels without a visual bloom. Traditionally, the presence of cyanotoxins at trace concentrations has been confirmed through time and resource-consuming methods which include liquid chromatography/tandem mass spectrometry (LC/MS/MS, EPA method 544) [11], high performance liquid chromatography (HPLC, EPA method 8315A) [12], and enzyme-linked immunosorbent assay (ELISA, EPA method 546) [13]. These methods have a good detection range of 0.1 to 2.5 μg L^{-1}, but they are time consuming and mostly conducted in a laboratory, often requiring expensive equipment and highly trained personnel. Therefore, it is urgent to develop a cost-effective, simple, and reliable cyanotoxin detecting tool to respond quickly during HAB events.

Biosensors have been proposed as an effective method to detect trace amounts of various emerging contaminants such as viruses [14], pharmaceuticals, antibiotics [15], and infectious

diseases [16]. Among many types of biosensors, bioelectrochemical detection can be a promising alternative to conventional methods due to its simplicity, readiness, and effectiveness. In bioelectrochemical MC-LR detection, the sensing technique heavily depends upon the affinity between the MC-LR dependent antibody and MC-LR molecules. It was previously discovered that MC-LR contains a unique structural feature, a β-amino acid (ADDA), which plays an important role in its toxicity as well as its recognition by ADDA-specific antibodies [17]. Many studies have reported the detection of MC-LR using monoclonal antibodies such as AD4G2 [18], IgG1 (e.g., mouse and goat)[19], and polyclonal antibodies [20]. However, most biosensors were fabricated using gold as a substrate or glass carbon electrodes (GCE), and often use nanoparticles (NPs) in order to increase the sensitivity [21-23] . Although there is a screen printed carbon electrode (SPCE) in conjunction with nano-Prussian blue-chitosan [24], it is expensive and challenging to construct. It is important to develop a cost-effective and simple biosensor to detect MC-LR in water.

In this study, an Anti-MC-LR/MC-LR/Cysteamine coated screen-printed carbon electrode (SPCE) biosensor was newly fabricated for the detection of MC-LR in real water samples using electrochemical impedance spectroscopy (EIS). Among many antibodies, a specific MC-LR monoclonal antibody (i.e., Anti-MC-LR) was selected due to its high sensitivity and selectivity [25]. The electron transfer properties of the cysteamine functionalized biosensor were investigated using cyclic voltammetry (CV). The surface nanolayer of the biosensor was characterized using scanning electron microscopy (SEM)-energy dispersive X-Ray spectroscopy (EDS) and X-Ray photoelectron spectroscopy (XPS). Following the characterization of the anti-MC-LR/MC-LR/cysteamine/SPCE biosensor, the functionality of the sensor's resistance to time and selectivity against other MCs and potentially interfering ions found in surface waters were thoroughly

investigated. Finally, the developed biosensor was tested to detect MC-LR in natural surface water samples and compared with previously reported similar methods.

1.2. Thesis Statement and Tasks

The overall objective of the study was to fabricate and investigate a novel Anti-MC-LR/MC-LR/Cysteamine/SPCE for the implementation of an easily operational, low-cost, and quick method for the determination of cyanotoxins in natural water systems. This will be accomplished with the following four tasks: 1) Preliminary analysis using screen-printed gold electrode (SPGE), 2) fabrication and characterization of Anti-MC-LR/MC-LR/Cysteamine/SPCE, 3) Analysis of Anti-MC-LR/MC-LR/Cysteamine/SPCE, and 4) Application to MC-LR detection in real surface water samples.

Task 1: Preliminary analysis using Screen Printed Gold Electrode (SPGE)

Based on the literature review, many papers report the use of a gold surface (including gold nanoparticles and SPGE). Therefore, in this task, an initial Anti-MC-LR/MC-LR/Cysteamine/SPGE was fabricated and characterized using CV and EIS measurements of each individual layer to demonstrate the technical feasibility of the fabrication process and electrochemical MC-LR detection.

Task 2: Fabrication and characterization of Anti-MC-LR/MC-LR/Cysteamine/SPCE

To further improve the cost of this novel detection method, the SPGE was switched out for a screen-printed carbon electrode (SPCE). In this task, the novel Anti-MC-LR/MC-LR/Cysteamine/SPCE was characterized using surface analysis, including SEM and XPS measurement, and electrochemical analysis was done using CV and EIS measurements of each layer in the developmental process.

Task 3: Analysis of Anti-MC-LR/MC-LR/Cysteamine/SPCE

In this task, the analytical performance of the Anti-MC-LR/MC-LR/Cysteamine/SPCE was evaluated. Fist, the calibration curves were developed and the limit of detection (LOD) was determined. Then, the sensor reproducibility and lifetime were assessed. Lastly, the selectivity and interference analysis were conducted with other MCs and potential interfering ions found in surface water.

Task 4: Application to MC-LR detection in real surface water samples

In this task, a real surface water sample was collected from a water body experiencing HABs and analyzed using the Anti-MC-LR/MC-LR/Cysteamine/SPCE. The sensor performance was compared to other similar analytical methods. MC-LR concentrations were validated using the enzyme-linked immunosorbent assay (ELISA, EPA method 546).

CHAPTER 2: LITERATURE REVIEW

2.1. Current Technologies

When testing a sample for MC-LR, the most widely used method is enzyme-linked immunosorbent assay (ELISA), method 546, (Figure 1). A single kit comes with a 96-well microtiter plate which is already coated with a microcystin-protein analogue. After being filtered with a 0.45 μm filter, 40 μL of the sample is added to the wells with the dilution buffer where the MC-LR binds to the microcystin-protein analogue already immobilized in the wells, then the MC-LR labeled with horseradish peroxidase (MC-LR-Px conjugate). After 20 minutes, an acid stop solution is added to stop the generation of the color. Using a plate reader, the optical density of the wells is measured using a wavelength of 450nm and the unknown MC-LR concentration of the sample is determined by comparing the value with a standard calibration curve developed from known concentrations. The detection range of the ELISA kit is between 0.1 and 2.5 μg L^{-1} [13]. The LOD of the ELISA kit is 0.1 μg L^{-1} .
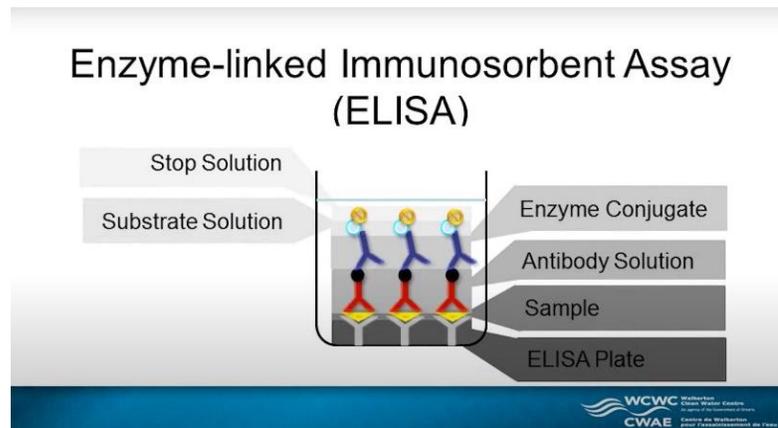
Figure 1. ELISA process [26].

The second most accepted method for detecting MC-LR is liquid chromatography/tandem mass spectrometry (LC/MS/MS), method 544. The LC/MS/MS requires a 500-mL water sample to be filtered using a 0.4 μm filter. The intracellular toxins are released from the cyanobacteria cells acquired on the filter by placing the filter in a methanol solution containing 20% reagent water for one hour at -20 ℃. The liquid is then collected off the filter and mixed back into the 500-mL filtrate. The combined sample is then passed through a solid phase extraction (SPE) cartridge to extract the MC-LR. A small amount of methanol containing 10% reagent water is used to remove the MC-LR from the SPE. Nitrogen is used to evaporate the water in the sample to concentrate the sample to a 1-mL volume. 10-μL of the sample is injected into the LC equipped with a C8 column that is interfaced to an MS/MS. The MC-LR is separated and identified by comparing the acquired mass spectra and retention times to references for calibration standards acquired under identical LC/MS/MS conditions. The concentration of MC-LR is determined by external standard calibration. The detection limit of the LC/MS/MS method is 4.3 ng L^{-1}. [11]

Table 1 summarizes and compares the two standard MC-LR detection methods discussed, LC/MS/MS and ELISA.

Table 1. *Comparison of Standard MC-LR Detection Methods*

	LOD	Working Range	Analysis time	Advantages	Disadvantages	Analysis price
ELISA	0.1 µg/L	0.1 - 2.5 µg/L	2 hrs	• Can analyase multiple samples at one time • High specifity and sensitivity	• Refrigerated transpotation and storage required • Sophisticated techniques • Expensive equipment	~ $20/sample
LC/MS/MS	4.3 ng/L	40 – 400 ng/L	1.5 hrs	• Low detection ability • Simple procedures	• Refrigerated transpotation and storage required • Sophisticated techniques • Expensive and bulky equipment	~$150/sample

The major component that pertains to the sensor's overall economic design is the screen-printed electrode (SPE) aspect. A SPE design allows for large-scale production, reduced costs, and yet high reproducibility. The overall minimal cost design makes for greater potential implementation. According to EPA's report titled "Water Treatment Optimization for Cyanotoxins", certified laboratory analysis costs can range up to $20 per sample for ELISA and $150 for LC/MS/MS [27]. This prosperous design mitigates the high cost for a quick response (e.g., less than $5 for one measurement). A sensor with high availability to the general community, within the US and globally, has the potential for maximum MCs detection awareness, the ultimate intention for this researched design.

2.2. Optical Detection

In a surface plasma resonance (SPR) biosensor, the sample is pumped over the surface of the sensor allowing for the measured component to bind to the surface. Light is used to reflect off the SPR chip and the resonance wavelength is measured in Resonance Units (RU), depending on the amount of the component that is bound to the surface of the chip, the measured reflected wavelength changes (**Figure 2**(a)). Herranz et al., 2010 [28] developed a sensor that allowed for the simultaneous detection of MC-LR in four different samples and could be regenerated up to 40 times. Chen et al., 2011 [29] developed a miniature SPR for field detection and could be regenerated 20 times. In both studies, it was determined that the best results could be obtained when the gold surface of the chip was modified based on MC-LR immobilization. Herranz et al., 2010 [28] used a carboxylic-SAM (oligo ethylene glycol alkanethiol) while Chen et al., 2011 [29] used a sulfhydryl-SAM (bovine serum albumin) layer to immobilize the MC-LR. It was found that

when the standard solutions of 50 µL of known concentration of MC-LR and the anti-body (MC-LR monoclonal antibody (MC10E7)) are pumped over the surface of the sensor at 25-30 µL/min, the free anti-body (not bound to the MC-LR in solution) will bind the immobilized MC-LR on the
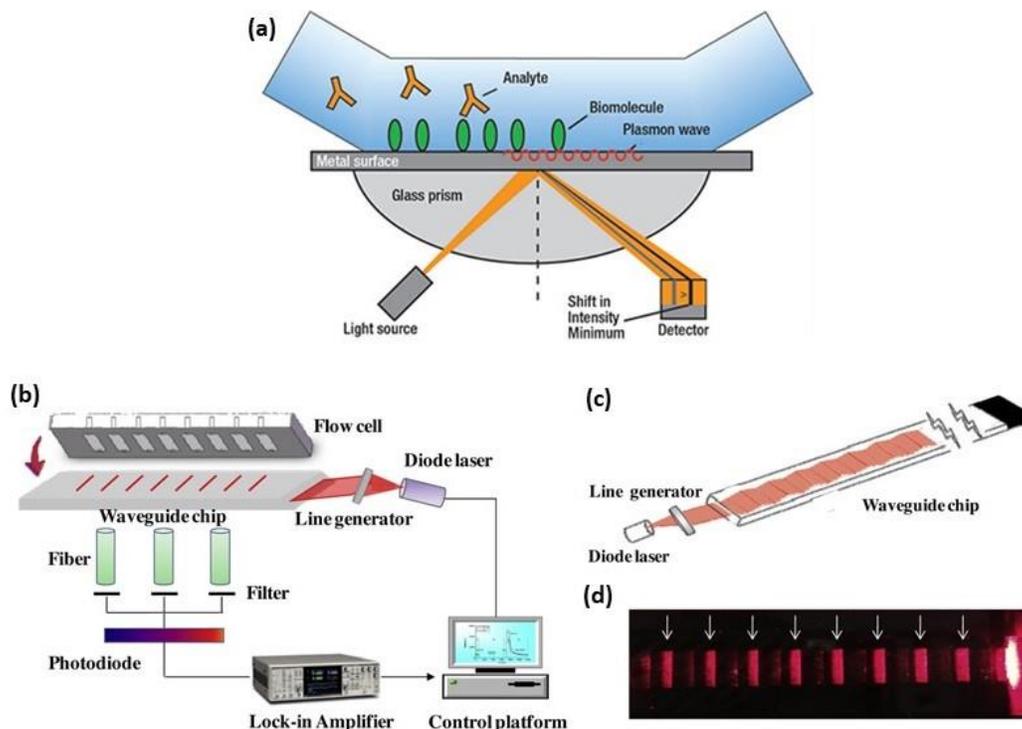
Figure 2. *(a) SPR biosensor [30]; (b) Fluorescence waveguide biosensor with a removable flow cell (c) Path taken by excitation light, and (d) Image of the waveguide chip [31]*

surface of the sensor resulting in a signal increase. The measured signal (RU) can then be normalized and compared against the varying concentrations of MC-LR in standard solutions to create a standardized curve which can then be used to determine the concentration of MC-LR in an unknown sample.

In a fluorescence waveguide biosensor, the excitation light from a diode laser (635 nm) provides energy which excites the fluorophores that are attached to the sensor. The emission from the fluorophore changes depending on how much of a component is bound to the surface, this signal change can be measured and compared to the concentration of the substance in solution (**Figure 2**(b-c)). A previous work conducted by Liu et al., 2017 [32], used a waveguide-based fluorescent immunosensor was developed to simultaneously test up to 32 contaminants, focusing on MC-LR, and can be regenerated 100 times. Herranz et al., 2012 [33], used an automated portable array biosensor was developed using microscope slides to simultaneously test six different samples and can be regenerated at least 15 times. Murphy et al., 2015 [34] performed an antibody-based optical-planar waveguide platform biosensor is developed to detect free MC-LR in a sample. In all the studies, MC-LR or a MC-LR conjugate was immobilized onto the surface of the chip and similarly to the SPR, the free antibodies in the solution bind to the antigen immobilized on the chip. The difference is that the antibodies used are Cy5.5-labeled MC-LR antibody [32, 33] or horseradish peroxidase (HRP)-labeled anti- hemagglutinin (HA) monoclonal antibody [34]. The difference in the reflected fluorescence signal is compared to the concentration of MC-LR in the sample to generate a standard curve. The sample sizes used in the literature have a range of 0.4 – 0.8 mL and a flow rate range of 0.3 – 1 mL/min [32-34].

2.3. Electrochemical Detection

The current most widely studied method for detecting MC-LR using a biosensor is to use electrochemical means. In this method, the target-aptamer is immobilized directly onto the surface of the electrode and measured utilizing a variety of electrochemical transduction techniques. Measurable changes in electrical output such as impedance (Ω), voltage (V) , and current (A) result from molecule interactions at the electrode surface [35]. Electrochemical sensors offer various advantages such as the ease of miniaturization, compatibility with innovative microfabrication technologies, quick response, simplicity, etc. [36]. There are a variety of electrode surface which can be used including glassy carbon electrode (GCE), screen printed electrodes (SPE), and carbon paste electrodes (CPE).
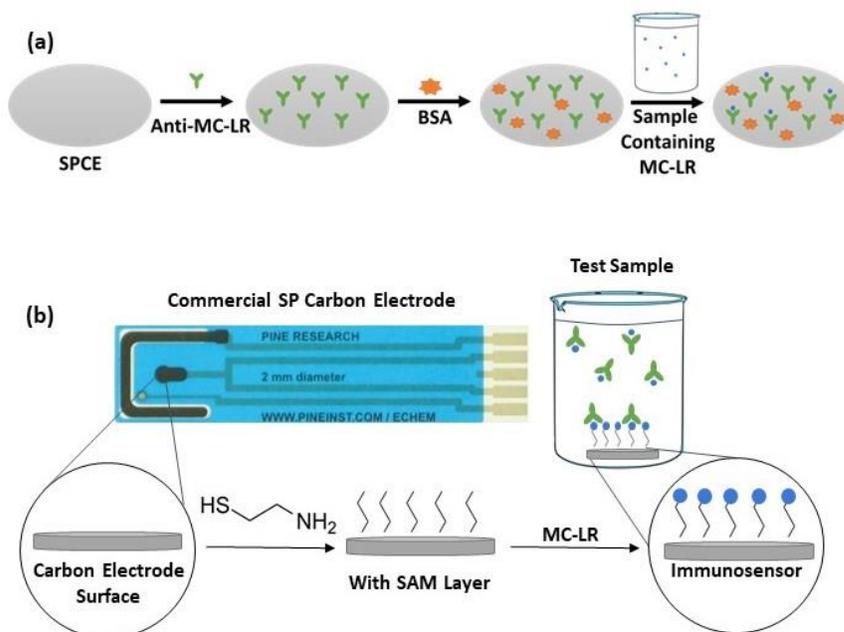
Figure 3. (a) Direct; surface functionalization of SPCE using antibody coating (b) Indirect; surface functionalization of the sensor and mechanism of carbon SPE coating with MC-LR.

There are two methods of electrochemical detection, direct and indirect (in this thesis) (**Figure 3**). The direct method uses an antibody bound to the surface to directly measure the amount of MC-LR in the sample. On the other hand, the indirect method uses MC-LR immobilized onto the surface of the electrode and mixes a fixed concentration of anti-body in the sample and then measure the amount the anti-body which binds to the MC-LR on the surface of the electrode (i.e., not bound in the sample). Previous studies [37, 38] have demonstrated the efficiency of both antibody-coated surfaces and an immobilized MC-LR molecule coating for the detection of MC-LR in water, however, the indirect method is more commonly studied due to a lower LOD.

Most focused research area is how to increase the sensitivity of the electrode. The most common ways are the addition of nanoparticles (NP) [39, 40] or an additional labeled antibody layer [24, 41]. NP can be used to increase the surface area of the electrode, allowing for more bonding locations of the analyte. The additional labeled antibody layer can be added as a final step onto the bound MC-LR (direct) or anti-MC-LR (indirect) from the sample measurement. This creates a larger structure to more dramatically change the measured resistance (EIS) or a specific chemical reaction more easily measured (DPV) in order to enhance the intensity of the output signal. A summary of the various reported working electrochemical biosensors for MC-LR detection and their methods are listed in **Table 2**.

2.3.1 Direct detection

The direct detection method uses an anti-body immobilized to the surface of the electrode to measure the amount of MC-LR in the sample. The addition of nanomaterial [23, 39, 42], an

additional labeled antibody layer [41, 42] or labeled MC-LR molecules [43, 44] can be used to increase the sensitivity of the sensor.

Thong et al., 2011 [39] used gold nanoparticles (AuNPs) to increase the sensitivity of a gold electrode coated with L-cysteine. The Anti-MC-LR was then immobilized onto the AuNPs which the MC-LR from the sample is then able to bind to. The MC-LR/Anti-MC-LR/Au NPs/L-cysteine/Au had a working range of 0.05 to 15.00 μg L^{-1} and a LOD of 20 ng L^{-1}.

Talamini et al., 2018 [45] developed an Anti-MC-LR/AuNP-BSA/Br-Py/GCE for the rapid detection of MC-LR. The glassy carbon electrode (GCE) was first modified with a film of liquid crystal (E)-1-decyl-4-[(4-decy-loxyphenyl)diazenyl] pyridinium bromide (Br-Py), then gold nanoparticles stabilized in bovine serum albumin (AuNP-BSA), and Anti-MC-LR. The MC-LR/Anti-MC-LR/AuNP-BSA/Br-Py/GCE had a linear range of detection of 0.05 to 500.0 pg L^{-1}, LOD of 0.05 pg L^{-1}, and was successfully tested in spiked seawater.

Zhang et al., 2017 [42] used the combination of a MoS$_2$ nanosheet and gold nanorods (AuNRs) to develop the surface of a gold electrode. After the layer of AuNRs, a layer of Anti-MC-LR is added to form the test ready anti-MC-LR/AuNRs/MoS$_2$/Au (**Figure 4**(a)). Then, the sample containing MC-LR is dropped onto the surface to bind with the Anti-MC-LR. Lastly, a horseradish peroxidase-labeled anti-MC-LR (HRP-Anti-MC-LR) is dropped onto the surface. The HRP-Anti-MC-LR then binds to the MC-LR from the sample which has bound to the surface of the electrode. HRP acts as a catalyst in the oxidation of H$_2$O$_2$ which can be measured by differential pulse voltammetry (DPV). The HRP-anti-MC-LR/MC-LR/anti-MC-LR/AuNRs/MoS$_2$/Au had a linear range of 0.01 to 20 μg L^{-1} and a LOD of 5 ng L^{-1}. The next year, the same group made a few modifications to the process to create an Au@Pt-anti-MC-LR/MC-LR/anti-MC-LR/AuNCs/MoS$_2$/Au sensor [46].
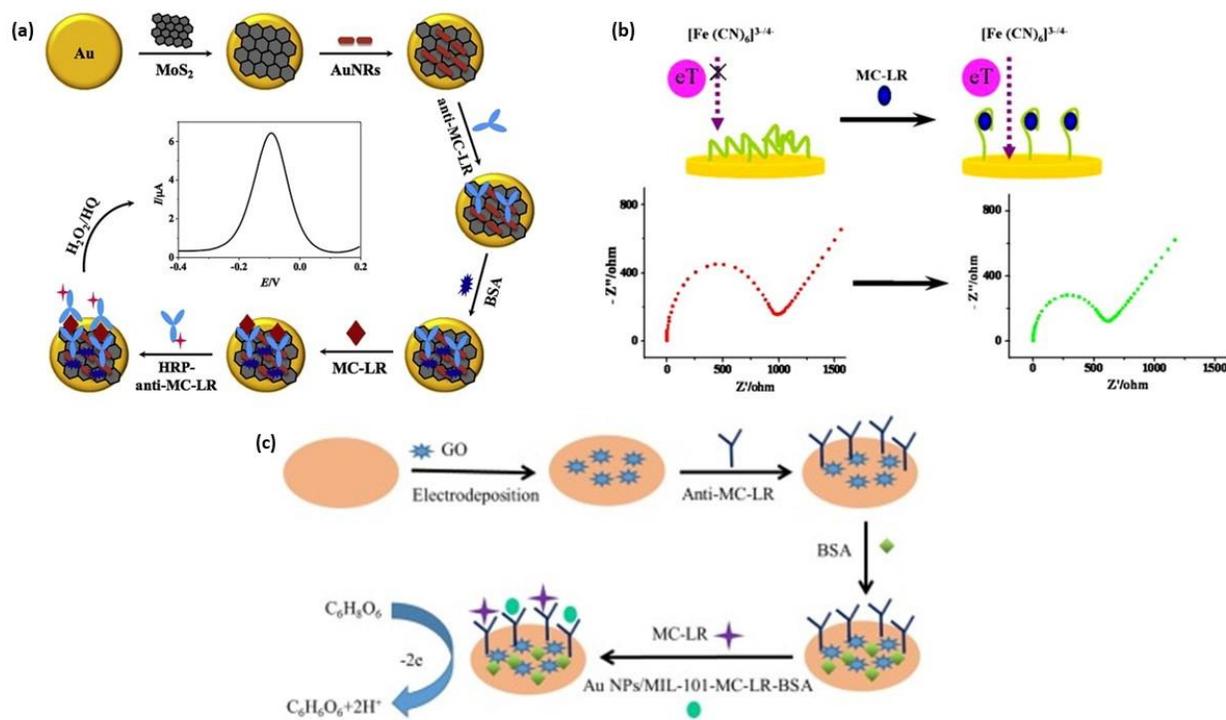
Figure 4. *Direct detection method using (a) an additional labeled antibody layer [42], (b) DNA [47], and (c) labeled MC-LR [43].*

Another way to increase sensitivity is by the addition of a labeled MC-LR molecule. For example, Zhang et al., 2019 [43] used a porous metal organic frameworks (MOFs) material (MIL-101) loaded with AuNPs (AuNPs@MIL-101) to label MC-LR-BSA (**Figure 4**(c)). The labeled MC-LR can be added to fill the spots which the MC-LR from the sample did not fill. Additionally, the development of the electrode included the electrodeposition of graphene oxide (GO) onto the surface of the GCE. The high conductivity and catalytic property of the GO and AuNPs@MIL-101 resulted in high sensitivity of the developed sensor with a detection range of 0.05 pg L^{-1} to 75 ng L^{-1} and LOD of 0.02 pg L^{-1}.

Another substrate that can be used for the direct detection of MC-LR is DNA. Zhang et al., 2018 [48] used Calf thymus DNA (ctDNA) and Lin et al., 2013 [47] used single-strand DNA

(ssDNA) to modify the surface of the electrode. Both studies used EIS as their measurement method for determination of the calibration curve. Due to the chain like structure of the DNA, it lays randomly folded on the electrode, and when the MC-LR from the sample interacts with the DNA, the DNA molecules lift up off of the surface of the electrode (not folded over anymore) which results in a decrease in resistance (**Figure 4**(b)). The ctDNA modified electrode [48] reported a linear range of 4 to 512 ng L^{-1} and a LOD of 1.4 ng L^{-1}, while the electrode modified with ssDNA [47] reported a linear range of 1.0×10^{-7} to 5.0×10^{-11} mol L^{-1} and LOD of 1.8×10^{-11} mol L^{-1}.

Also using ssDNA, Bilibana et al., 2016 [23], modified a GCE using cobalt(II) salicylaldiimine metallodendrimer (SDD–Co(II)) as the substrate for the immobilization of silver nanoparticles (AgNPs). Then, MC-LR 5′-thiol ssDNA aptamer (MC-LR-A) is immobilized onto the AgNPs to create binding sites for the MC-LR in the sample. The MC-LR/MC-LR-A /AgNPs/SDD–Co(II)/GCE used CV analysis to create a calibration curve with a detection rage of 0.1 to 1.1 µg L^{-1} and LOD of 0.04 µg L^{-1}.

2.3.2 Indirect detection

The indirect detection method uses MC-LR immobilized onto the surface of the electrode and mixes a known concentration of anti-body in the sample and then measures the amount the anti-body which binds to the MC-LR on the surface of the electrode (i.e., not bound in the sampler). Similar to the direct detection method, the addition of nanomaterial [49] or an additional labeled antibody layer [21, 24] can be used to increase the sensitivity of the sensor.

Dos Santos, et al., 2019 [50], developed a novel portable electrochemical sensing system. The system consisted of a sample processing module and detection module. The detection module included 8 independent modified MC-LR/Cysteamine/Au electrodes for multiple samples. EIS was used for the analysis of the sensor, with a linear dynamic range of 3.3×10^{-4} to 10^{-7} g L^{-1} and a LOD of 5.7×10^{-10} g L^{-1}. The incorporation of the processing module, not only allowed for the detection system to be portable, but also allowed for the simultaneous detection of free and total MC-LR. The system was successfully implemented into a freshwater system.

One example of the addition of an antibody layer is the Goat-anti-rabbit(IgG-HRP)/Anti-MC-LR/MC-LR antigen/PB-CS/SPCE developed by Guan, et al., 2019 [24]. This developmental process used the addition of the Goat-anti-rabbit (IgG-HRP) to increase the current signal for more clearly defined peaks. The sensor was connected to a smartphone-controlled electrochemical analyzer for point-of-need detection (**Figure 5**(a)). The sensor was analyzed using CV to have a working range of 0.001 to 100 μg L^{-1} with a LOD of 0.11 ng L^{-1}.
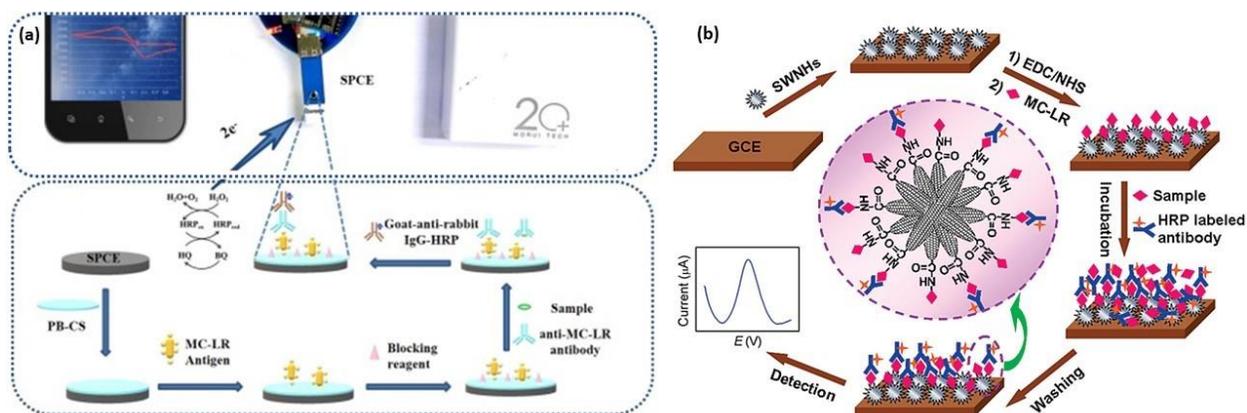
***Figure 5.** Indirect detection method using (a) an additional labeled antibody [24] and (b) single-walled carbon nanohorns (SWNHs) [49].*

Hou et al., 2016 [21] used a labeled antibody as well as AuNPs. The labeled antibody used was horseradish peroxidase-labeled monoclonal anti-MC-LR (HRP-mAb) to amplify the impedimetric signal. A GCE base was used, modified with AuNPs, then a cysteamine-glutaraldehyde solution created a surface for the MC-LR-bovine serum albumin (MC-LR-BSA) to immobilized and lastly, the HRP-mAb was competitively bound to the MC-LR-BSA. The HRP-anti-MC-LR/MC-LR-BSA/cysteamine-glutaraldehyde/AuNPs/GCE had a dynamic linear range of 0.01 to 100 μg L^{-1} with a LOD of 4 ng L^{-1}. The sensor was successfully implemented for the analysis of lake samples.

Zhang et al., 2016 [22], immobilized MC-LR onto a GCE using carbon nanofibers (CNFs) and polyethylene glycol (PEG) film. A second antibody, goat anti-mouse IgG, combined with AuNPs was used. When the sensor was immersed in a HCl solution, the AuNPs electro-oxidized to form AuCl$_4^-$ which is measured using DPV. The AuNPs-Ab$_2$/anti-MC-LR/MC-LR/PEG/CNFs/GCE had a 0.0025 - 5 μg L^{-1} with a LOD of 1.68 ng L^{-1}.

Zhang et al., 2010 [49], used single-walled carbon nanohorns (SWNHs) to functionalize the surface of a GCE (**Figure 5**(b)), allowing for more carboxylic groups for the MC-LR to covalently bond to. Then, a HRP labeled Anti-MC-LR competitively bonds to the MC-LR in the sample and the MC-LR on the surface of the electrode. Similarly to Zhang et al., 2017 [42], the HRP label acts as a catalyst for the oxidation of o-phenylenediamine (o-PD) by H$_2$O$_2$ to 2,2′-diaminoazobenzene, which can then be measured with DPV. The detection ranging and LOD of the sensor was analyzed to be 0.05 - 20 μg L^{-1} and 0.03 μg L^{-1}, respectively. The HRP-Anti-MC-LR/MC-LR-SWNHs/GCE was successfully applied to the detection of MC-LR in lake water without the need of any pretreatment.

More recently, Gan et al., 2022 [51], used a screen printed carbon electrode (SPCE) modified with hydrogel@polydopamine (GH@PDA), to create additional functional groups for the immobilization of MC-LR modified AgNPs. Then, Anti-MC-LR competitively binds to the MC-LR-Ag, and a multi-HRP-(MCSs/Thi@AuNPs)-Ab_2, where Ab_2 is a HRP-labeled secondary goat anti-rabbit antibody, binds to the Anti-MC-LR and measured using CV. The detection range and LOD of the multi-HRP-(MCSs/Thi@AuNPs)-Ab_2/MC-LR-Ab_1/MC-LR-Ag/GH@PDA/SPCE is 0.01 to 10 μg L^{-1} and 9.7 ng L^{-1}, respectively.

Table 2. Comparison of modified biosensors for electrochemical detection of MC-LR

Modifier	Analyte	Direct vs. Indirect	LOD	Mode	Sample	Ref.
MC-LR/ctDNA/Au	MC-LR	Direct	1.4 ng/L	EIS	Tap and lake water	[48]
MC-LR/ssDNA/Au	MC-LR	Direct	18 ng/L	EIS	Lake, river, and tap water	[47]
MC-LR/MC-LR-A/AgNPs/SDD–Co(II)/GCE	MC-LR	Direct	40 ng/L	CV	Freshwater and environmental samples	[23]
HRP-anti-MC-LR/MC-LR/BSA/anti-MC-LR/AuNR/MoS$_2$/Au	HRP-anti-MC-LR	Direct	5 ng/L	DPV	Lake, tap, and drinking water	[42]
Au@Pt-anti-MC-LR/MC-LR/anti-MC-LR/AuNCs/MoS$_2$/Au	Au@Pt-anti-MC-LR	Direct	0.3 ng/L	DPV	Lake, tap, and drinking water	[46]
MC-LR/Anti-MC-LR/AuNPs/L-cysteine/Au	MC-LR	Direct	20 ng/L	DPV	Lake, tap, and mineral water	[39]
MC-LR-HRP/MC-LR/Anti-MC-LR/SPGE	MC-LR-HRP	Direct	0.1 ng/L	CV	River water	[44]
MC-LR/anti-MC-LR/AuNP-BSA/Br-Py/GCE	MC-LR	Direct	0.05 ng/L	EIS	Spiked seawater	[45]
Pt$_{70}$Ru$_{30}$-Ab$_2$/MC-LR/BSA/GS-Ab$_1$/GCE	Pt$_{70}$Ru$_{30}$-Ab$_2$	Direct	9.63 ng/L	CV	Polluted water	[41]
AuNPs@MIL-101 labeled-MC-LR-BSA/MC-LR/BSA/Anti-MC-LR/GO/GCE	Au NPs@MIL-101 labeled-MC-LR-BSA	Direct	20 ng/L	CV	Lake water	[43]

Modifier	Analyte	Direct vs. Indirect	LOD	Mode	Sample	Ref.
MC-LR/Anti-MC-LR/AgNP/Thiourea SAM/Au	MC-LR	Direct	0.007 ng/L	Capacitance	Bottled, tap, well, reservoir, pond water	[52]
MC-LR/BSA/Anti-MC-LR/AuNP/L-cysteine/Au	MC-LR	Direct	18.2 ng/L	EIS	Bottled water	[40]
Anti-MC-LR/MC-LR/Cysteamine/Au	Anti-MC-LR	Indirect	0.57 ng/L	EIS	Lake water	[50]
Goat-anti-rabbit(IgG-HRP)/Anti-MC-LR/MC-LR antigen/PB-CS/SPCE	Goat-anti-rabbit(IgG-HRP)	Indirect	0.11 ng/L	CV	Spiked tap, reservoir, and lake water	[24]
HRP-anti-MC-LR/MC-LR-BSA/cysteamine-glutaraldehyde/ AuNPs/GCE	HRP-anti-MC-LR	Indirect	4 ng/L	EIS	Lake water	[21]
AuNPs-Ab$_2$/Anti-MC-LR/MC-LR/PEG/CNFs/GCE	AuCl4-	Indirect	1.68 ng/L	DPV	Lake water	[22]
HRP-Anti-MC-LR/MC-LR-SWNHs/GCE	HRP-anti-MC-LR	Indirect	30 ng/L	DPV	Lake water	[49]
multi-HRP-(MCSs/Thi@AuNPs)-Ab$_2$/MC-LR-Ab$_1$/MC-LR-Ag/GH@PDA/ SPCE	multi-HRP-(MCSs/Thi@AuNPs)-Ab$_2$	Indirect	9.7 ng/L	CV	Lake water	[51]
Anti-MC-LR/MC-LR/Cysteamine/SPCE	Anti-MC-LR	Indirect	0.23 ng/L	EIS	Lake water	This Study

CHAPTER 3: MATERIALS AND METHODS

3.1. Chemicals and Reagents

Cysteamine (Cat. No. M9768) was purchased from Sigma Aldrich (St. Louis, MO, USA). Sodium phosphate monobasic monohydrate (NaH_2PO_4) (Cat. No. 389872500), sodium phosphate dibasic (Na_2HPO_4) (Cat. No. 424375000), phosphate buffer saline (PBS) (Cat. No. 10010031), potassium Ferricyanide (Cat. No. 196785000), sulfo-NHS (N-hydroxysulfosuccinimide) (Cat. No. 24510), N-(3-(dimethylamino)propyl)-N′-ethylcarbodiimide hydrochloride (Cat. No. 22980), sodium chloride (Cat. No. AC447302500), calcium sulfate ($CaSO_4$, Cat. No. AA33301A7), cupric sulfate ($CuSO_4$, Cat. No. 7758998), and magnesium chloride ($MgCl_2$, Cat. No. LC163801) were purchased from Thermo Fisher Scientific (Waltham, MA, USA). MC-LR (Cat. No. ALX-350-012-C100), anti-MC-LR monoclonal antibody (MC10E7, lgG1 type, ALX-804-320-C200), MC-YR (Cat. No. ALX-350-044-C025), and MC-RR (Cat. No. ALX-350-043-C050) were purchased from Enzo Life (Farmingdale, NY, USA). The Abnova™ MC-LR ELISA kit (Cat. No.89028336) was purchased from Thermo Fisher Scientific (Waltham, MA, USA). The ELISA kit was analyzed using a VersaMax microplate reader (Molecular Devices, San Jose, CA, USA).

0.01 M phosphate buffer solution (PB, pH 7.6) was prepared by mixing solutions of NaH_2PO_4 and Na_2HPO_4 in Milli-Q water. The electrolyte solution was prepared by mixing 5 mM $[Fe(CN)_6]^{3-/4-}$ in 10 mM PBS solution (pH 7.3).

3.2. Anti-MC-LR/MC-LR/Cysteamine/SPCE Biosensor Fabrication
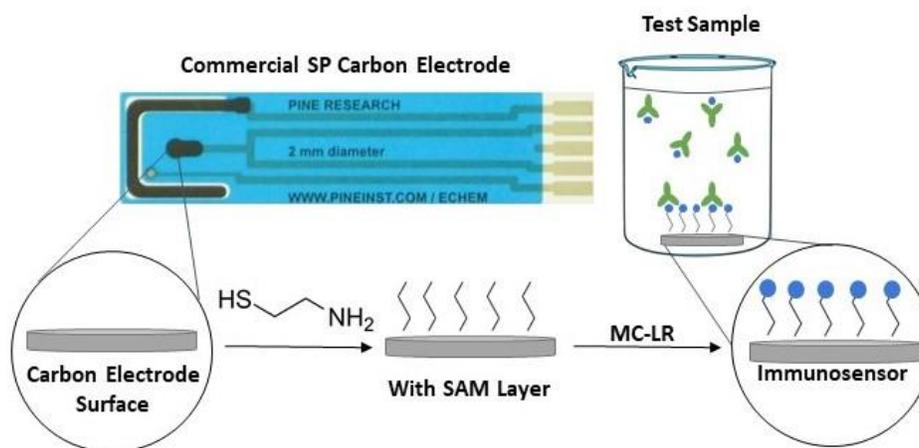
Figure 6. *Surface functionalization of the Anti-MC-LR/MC-LR/Cysteamine/SPCE biosensor surface and mechanism for the SPCE coated with MC-LR molecules.*

The surface functionalization process of the Anti-MC-LR/MC-LR/Cysteamine/SPCE biosensor is shown in **Figure 6**. First, the screen-printed carbon electrode (SPCE) (RRPE1001C, Pine Research Instrumentation Inc., Durham NC, USA) was sufficiently cleaned by pouring a small amount (approximately 10 mL) of acetone (99.7%, Cat. No. 180349, Thermo Fisher Scientific, Waltham, MA, USA) into individual 50 mL graduated polypropylene centrifuge tubes (Cat. No. 14375150, Thermo Fisher Scientific, Waltham, MA, USA), so that the working electrode (WE) was then completely submerged into the solution. With the lid, the tubes were placed in a large beaker with water and a probe-type ultrasonic bath (CL-334, No. 2015060673, Fisher Scientific), making sure none of the tubes were touching either the walls of the beaker or the probe. With a power of 500 watts and a frequency of 20kHz at an amplitude of 25%, the sensors were sonicated for 90 minutes at room temperature. Then, the sensors were removed and rinsed with 70% isopropanol and Milli-

Q water. The sensors were placed in a petri dish with a task wiper (Kimwipes) and dried with N_2 (99.999%). Next, a cysteamine self-assembled monolayer (SAM) was coated onto the surface of the carbon WE to provide anchoring sites for the MC-LR molecules [50]. For the SAM coating, 3 μL of 18 mM cysteamine, diluted using Milli-Q water, was dropped onto the surface of the WE. The sensors were then placed in a dark and semi-humid environment. After 4 hours, the electrode was rinsed with Milli-Q water and dried with N_2. To immobilize the MC-LR onto the SAM layer of the WE surface, the WE was incubated with an activated solution of MC-LR. The MC-LR was activated by using equal portions of 20 mM sulfo-N-hydroxysulfosuccinimide (sulfo-NHS), 80 mM N-(3-(dimethylamino)propyl)-N′-ethylcarbodiimide hydrochloride (EDC), and 10^{-2} g L^{-1} of MC-LR and spun in the centrifuge (Cat. No. 367160, Beckman Counlter, Inc. (Brea, CA)) at room temperature for 30 min at 500 rpm. Using a pipette, 1 μL of the activated MC-LR solution was dropped onto the WE and allowed to immobilize overnight in the refrigerator (4°C). The sensor was then rinsed with Milli-Q water and dried with N_2. The fabricated MC-LR detection biosensor was stored in the refrigerator before use (i.e., antibody application to test water samples).

3.3. Electrochemical Characterization of the MC-LR Detection Biosensor

The electrochemical characterization of the functionalization process of the Anti-MC-LR/MC-LR/Cysteamine/SPCE biosensor was conducted using EIS and CV measurements performed by the PalmSens 4 (Houten, Netherlands). Electrochemical characterization was conducted in three-electrode system using a modified Anti-MC-LR/MC-LR/Cysteamine/SPCE biosensor as the working electrode (WE), carbon counter electrode, and an Ag/AgCl reference electrode (MI-401, Microelectrodes, Inc., Bedford, NH, USA). The CV and EIS measurements were analyzed for each

step of the functionalization process, bare SPCE, cysteamine/SPCE, and MC-LR/cysteamine/SPCE, and compared to ensure electrode surface functionalization. For the EIS measurements, the potential of the DC and AC were set to 0.001V and 0.25V, respectively, and a frequency range of 0.01 to 100,000 Hz. For the CV measurements, the t equilibrium was set to 8 seconds, the E begin was -1.0 V, E step was 0.01 V, and the scan rate was 0.05 V s^{-1}.

3.4. Surface Characterization of the MC-LR Detection Biosensor using SEM and XPS

Surface structures of the fabricated biosensors were obtained with an Ultra 55 scanning electron microscopy (SEM) (ZEISS, Oberkochen, Germany). To characterize the surface chemical states, X-ray photoelectron spectroscopy (XPS) was performed with a Thermo Scientific ESCALAB Xi+ X-ray Photoelectron Spectrometer Microprobe (Thermo Scientific™, Massachusetts, USA) with a twin-crystal, micro-focusing monochromator and an Al anode. The XPS analysis chamber during measurement was held at a pressure below 1.0×10^{-7} torr. All spectra were calibrated to the carbon 1s peak, set to 284.8 eV.

3.5. MC-LR Detection using Fabricated Anti-MC-LR/MC-LR/Cysteamine/SPCE Biosensor

The analytical performance of the biosensor was tested using varying known concentrations of MC-LR. The monoclonal antibody (anti-MC-LR) was used because of its high sensitivity and selectivity toward MC-LR [25]. MC10E7 is very stable and exhibits low interferences from humic

acid, salts, and surfactants/organic solvents present in solutions [53], proving it well-suited for its application in a blend of water matrices.

Samples containing concentrations of MC-LR from 10^{-7} to 10^{-4} g L^{-1} were mixed with equal volumes of 10^{-2} g L^{-1} Anti-MC-LR and PB (pH 7.6) using the centrifuge at room temperature for 30 min at 500 rpm. This allows for sufficient time for the antibody to bind to the MC-LR in the sample. 1 μL of the sample was then dropped onto the working electrode and let sit, in the closed petridish, for an hour at room temperature to allow the available antibody molecules left in solution (not bound to the MC-LR molecules present in the sample) to bind to the MC-LR molecules on the surface of the sensor. The electrode was rinsed with Milli-Q water and then incubated with PB solution for a couple minutes. The sensor was then tested in the redox probe solution (0.005 M [Fe(CN)$_6$]$^{3-/4-}$ in PBS) using the PalmSens 4 to obtain EIS graphs. The total whole process including mixing antibody in the test solution and incubating the sensor took approximately less than 90 mins. The peak values (Z_{max}) were obtained from the EIS graph to create the standard curve. The EIS Nyquist plot curves were fitted to the appropriate circuit model using EIS Spectrum Analyser software (ABC Chemistry).

The limit of detection (LOD) was calculated using the following equation (1) [54].

$$LOD = k\frac{S_b}{b} \qquad (1)$$

where k is the parameter whose value is suggested to be 3 by the International Union of Pure and Applicable Chemistry (IUPAC), S_b is the standard deviation of blank signals and b is the slope of the calibration curve.

The reproducibility of the Anti-MC-LR/MC-LR/Cysteamine/SPCE biosensor was tested by preparing new test solutions and comparing to the previously developed standard curve.

3.6. Selectivity and Interference Tests

The selectivity of the biosensor toward MC-LR was evaluated by testing the cross-reactivity with other common MCs (MC-RR and MC-YR) [55]. Samples were prepared with a fixed concentration of 10^{-5} g L^{-1} of MC-LR, MC-RR, and MC-YR, as well as a combination sample of three MCs (i.e., MC-LR, MC-RR, and MC-YR).

The interference resilience of the biosensor was also analyzed by adding possible interfering ions commonly found in natural water to the MC-LR test sample. The ions selected for analysis were Na$^+$, Mg^{2+}, Cu^{2+}, Ca^{2+}, Cl$^-$, and SO$_4^{2-}$. In fresh surface water, sodium (Na$^+$) concentrations typically range between zero and 100 mg L^{-1}, magnesium (Mg^{2+}) concentration range is 1–100 mg L^{-1}, calcium (Ca^{2+}) concentration range is 1–135 mg L^{-1}, copper (Cu^{2+}) concentration range is 0.5–1,000 µg L^{-1}, chloride (Cl$^-$) concentration range is 1–100 mg L^{-1}, and sulfate (SO$_4^{2-}$) concentration averages 53 mg L^{-1} [56-60]. Keeping the ion concentrations within the typical ranges of natural surface water, the chemical concentrations selected were 82.4 mg L^{-1} NaCl, 143.4 mg L^{-1} MgCl$_2$, 3.93 mg L^{-1} CuSO$_4$, and 53.7 mg L^{-1} CaSO$_4$. 10^{-5} g L^{-1} of MC-LR was tested with the selected concentration of each chemical. A sample was also tested with a mixture all the chemicals.

3.7. Anti-MC-LR/MC-LR/Cysteamine/SPCE Biosensor Application to MC-LR Detection in Real Surface Water Samples

A natural surface water sample was collected from the Daecheong Lake in South Korea experiencing HAB events (**Figure 7**). The sonication method [61] was used to lyse the cyanobacteria, ensuring the MC-LR concentrations in the test sample. A CO-Z ultrasonic cleaner (PS-10A, AC100-120V, 60Hz) was used to sonicate the cyanobacteria for 30 minutes. The sample was then filtered using a glass fiber prefilter (No. APFA04700, MilliporeSigma, Burlington, MA, USA) to remove the larger particles and then a 0.22 μm membrane filter (No. SLGPM33RS, MilliporeSigma, Burlington, MA, USA) was used to remove the remaining particles. The MC-LR concentration was measured using ELISA (EPA method 546) [13] (APPENDIX D: ELISA PROCEDURES).
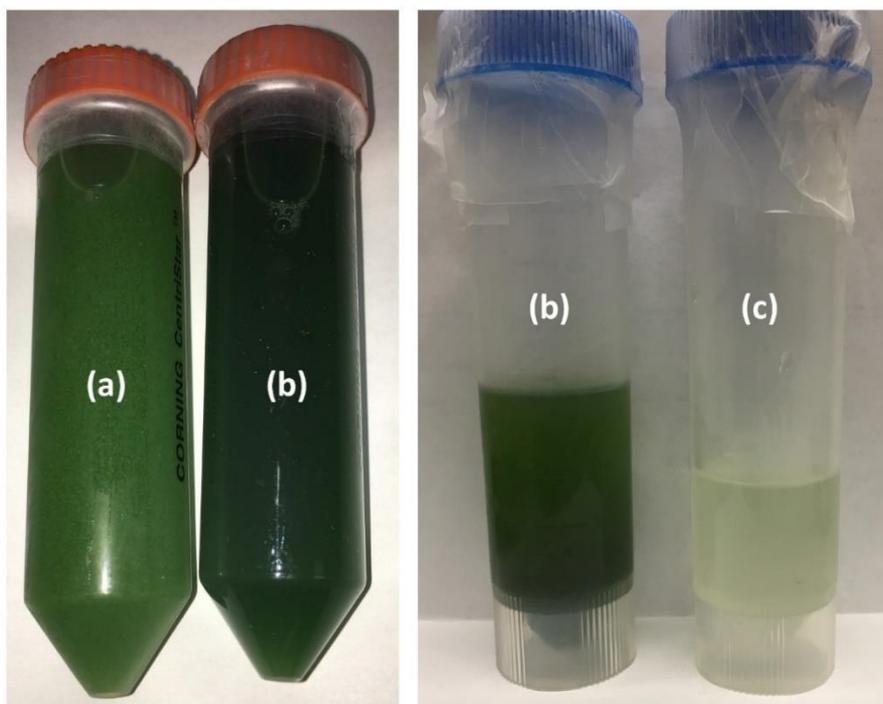
Figure 7. *Real surface water sample (a) initial sample; (b) sample after sonication; (c) sample after filtration.*

CHAPTER 4: RESULTS AND DISCUSSION

4.1. Surface Characterization of the Fabricated MC-LR Detection Biosensors

SEM was used to investigate the surface morphology of the electrodes after each step of the sensor surface functionalization (**Figure 8**). The bare SPCEs exhibited flakelike carbon structures, several microns in size, accompanied by smaller structures on their surface. These smaller structures include fibers and particles, attributed to polymer binders and fragmented carbon structures typical of electrode fabrication. After each step, the surface modification showed no significant alteration to the structure at the microscale. The density of particle and fibrous structures on the surface seemed to vary, attributed to the commercial SPE fabrication process. No discernible changes can be seen at this scale after functionalization, with surface modifications occurring solely at the nanoscale. All resulting changes to the electrode properties are then attributed to the surface functionalization.
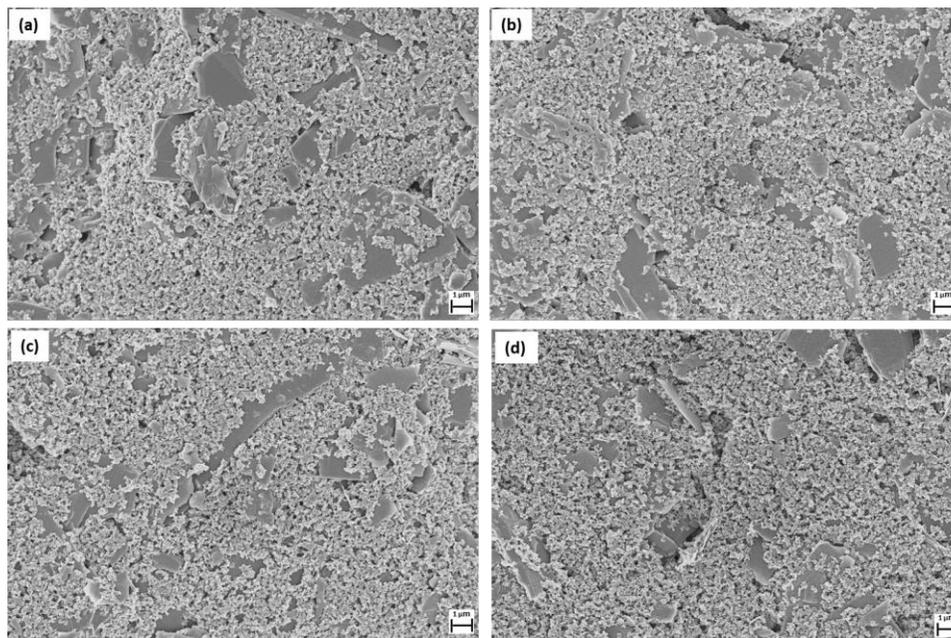
Figure 8. *Surface characterization of the development of the SPCE biosensor: (a) bare carbon (b) Cysteamine/SPCE (c) MC-LR/Cysteamine/SPCE (d) Anti-MC-LR/MC-LR/Cysteamine/SPCE.*

XPS confirmed the surface chemical states of the electrodes after surface modification. From the survey spectra and deconvoluted high-resolution spectra, deconvolution of the C 1s and N 1s core-level peaks confirms changes to the chemical states of the surface through the fabrication process (**Figure 9**(a)). Consistent among all C 1s spectra was presence of the C-C bond peak at 284.8 eV, which was the dominant peak in all electrodes (**Figure 9**(b)). The origin of this peak is from adventitious carbon as well as C-C bonds in coatings on the electrodes. A shorter peak from the C=C moiety at 284.3 eV, which originating from aromatic carbon of the electrode, was often present. After the coating with cysteamine (i.e., SAM), the signal increased in the region associated with bonds to heteroatoms such as C-N or C-S bonds (**Figure 9**(b)) [62]. Following attachment both of MC-LR and Anti-MC-LR, the spectra exhibited C-N and C-O bonds, however showed a signal consistent with amide bonding at 288.4 eV [63]. The electrode after adhesion of Anti-MC-LR did not show the presence of C=C bonding in the deconvolution, likely due to a thickness of the adsorbed layer, where the signal of the carbon electrode was no longer detected as XPS only probes the ~10 nm into the surface [64].

The N 1s peaks were also deconvoluted to determine the state of nitrogen on the electrode surface (**Figure 9**(c)). In the bare carbon electrode, the XPS indicated charged nitrogen species associated with the peak at ~402.4 eV [65]. The complex signal likely originated from the binding agents applied in commercial electrode fabrication, which can contain charged species such as quaternary nitrogen.[66, 67] With addition of the SAM coating on the electrode shows the emergence of new peaks, with a shoulder often associated with aromatic nitrogen [68], indicating a change to the electrode surface chemistry. After attachment of the MC-LR, the most prominent peak in the signal appeared at 399.8 eV, indicating the presence of amide bond formation consistent with the chemical structure. MC-LR has several nitrogen containing functional groups

(e.g., amides and guanidine) that further convolute the spectra. After the attachment of Anti-MC-LR, the peak shifts to 400.0 eV, attributed to primary amide bonds, with the shoulders associated with nitrogen in a variety of protonated states [69]. As was seen in the C 1s spectra, the initial peaks in the N 1s spectra associated with the electrode signal at 402.4 eV are no longer detected after the surface modification process.
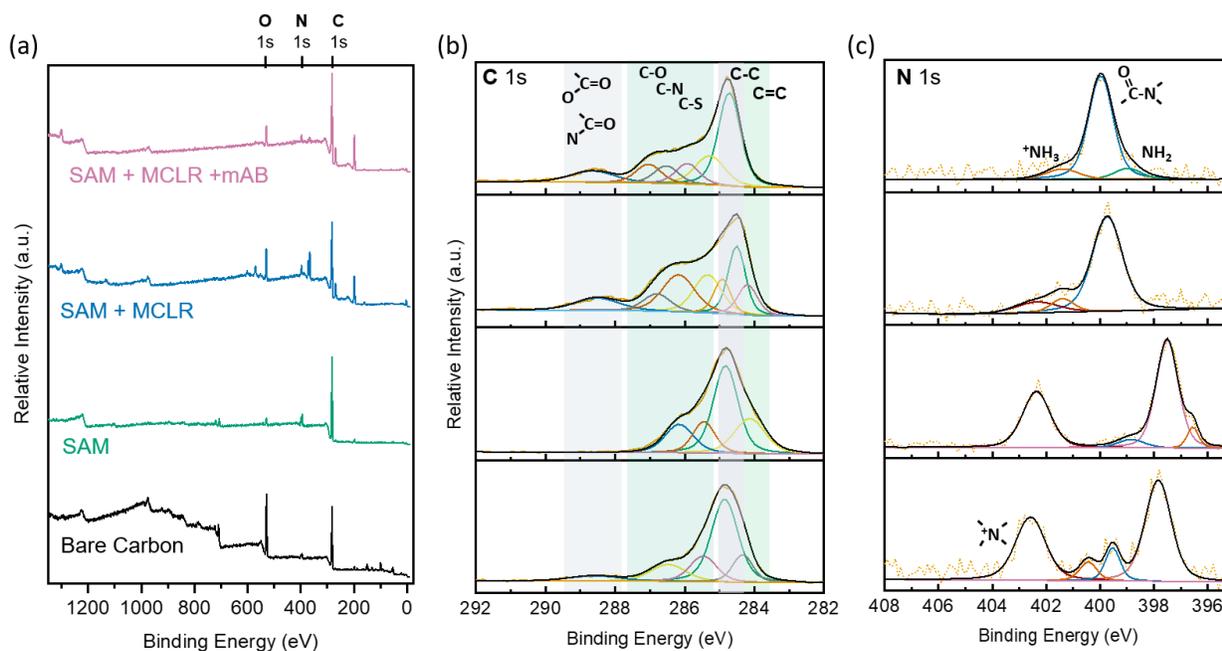

Figure 9. *(a) XPS survey spectra of the SPE through each step of the fabrication process. (b-c) High-resolution spectra of the C 1s and N 1s regions for each step. SAM: Cysteamine self-assembled monolayer, mAB: monoclonal antibody.*

4.2. Anti-MC-LR/MC-LR/Cysteamine/SPCE Biosensor Electrochemical Characterization

The electrode functionalization of the Anti-MC-LR/MC-LR/Cysteamine/SPCE biosensor was evaluated through the redox behavior of the cysteamine monolayer (i.e., SAM) by CV measurements using the redox probe solution via different substrate layers (**Figure 10**(a)). The highest redox peak current (27 μA) was observed with the SAM layer, which was attributed to the improvement in electron transport due to an electrostatic attraction between the positively charged cysteamine monolayer and the negatively charged redox probe solution [70]. A slight decrease to 20 μA was observed with the addition of the MC-LR, suggesting that binding of the MC-LR acted as a charge insulator from the probe solution and in turn decreases the current response. Lower redox peak (6 μA) was observed for the bare carbon electrode due to the hindrance of electron transport because of the absence of the SAM layer on the working electrode.

The Nyquist plots shown in **Figure 10**(b) were fitted with equivalent circuit models using EIS operation parameters including 0.5 mV and 0.25 V for the DC (direct current) and AC (alternating current), respectively, and a frequency range of 0.01 Hz – 100 kHz. The bare carbon electrodes (i.e., SPCE) showed the highest peak value of 14 kΩ, indicating the high barrier of electron transfer. The formation of the cysteamine SAM on the electrode generated a layer of high electrostatic attraction [70] which led to a decrease in the peak value to 1.4 kΩ. The immobilization of the MC-LR onto the cysteamine SAM resulted in an increase in the resistance, shown by a higher peak value of 8.7 kΩ on the Nyquist plot, which is in agreement with the result of the CV (**Figure 10**(a)).
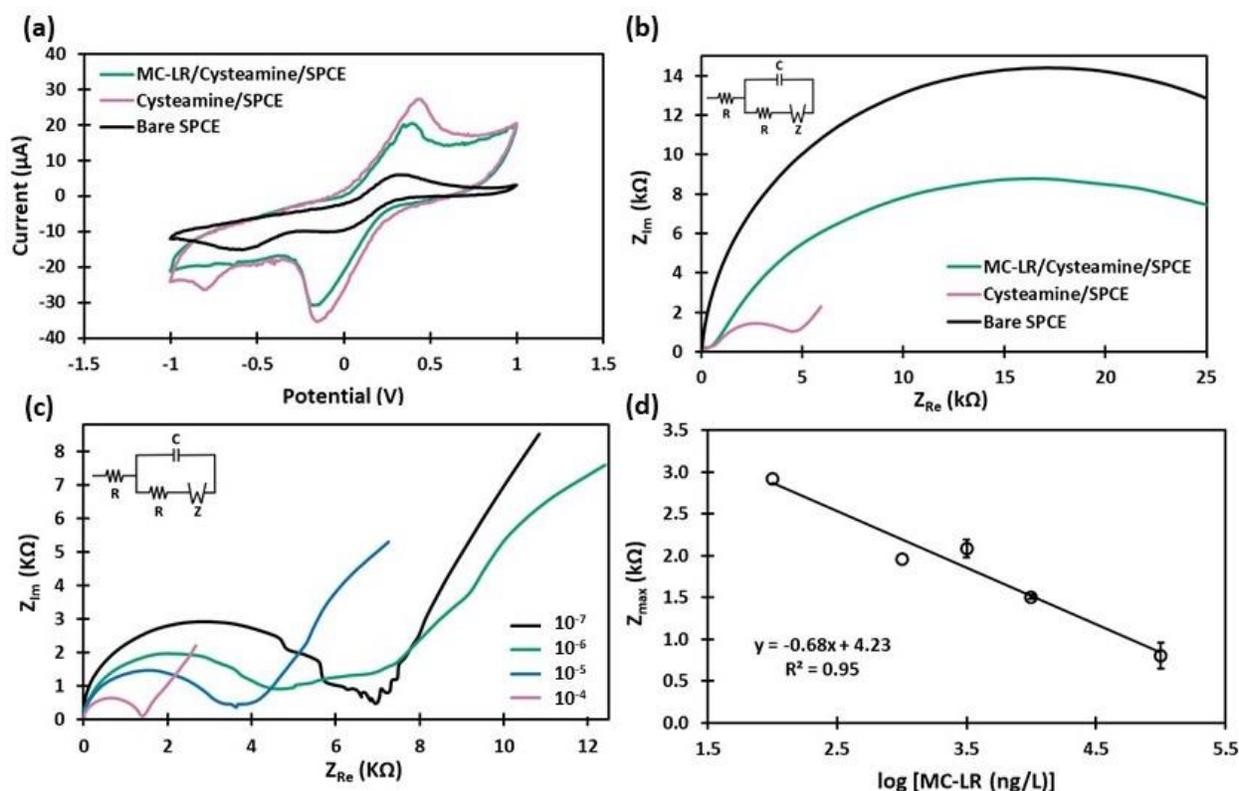
Figure 10. *Anti-MC-LR/MC-LR/Cysteamine/SPCE biosensor for MC-LR detection: (a) CV curves (b) Nyquist plots with different fabrication stages of the sensors (c) Nyquist plots with different MC-LR concentrations (d) Standardized curve for varying MC-LR test samples with error bars.*

4.3. Analytical Performance of Anti-MC-LR/MC-LR/Cysteamine/SPCE Biosensor

4.3.1. Calibration Curve and LOD

The purpose of this study was to develop and characterize a cost-effective and simple check for MC-LR in water, based on EIS, using a modified SPCE. The detection strategy was based on an indirect measurement of electron-transfer resistance on the biosensor surface [37, 38] where MC-LR was covalently immobilized using a cysteamine SAM, and the antibody binding to the MC-LR modified surface was competitively inhibited by MC-LR present in the sample.

EIS measurements were further carried out to characterize the binding between immobilized MC-LR and the anti-MC-LR monoclonal antibody. The variation in the electron-transfer resistance with different concentrations of MC-LR (10^{-7}–10^{-4} g L^{-1}) was evaluated using EIS and a calibration curve was created, where the higher the concentration of MC-LR in the test solution, the lower the number of antibody molecules that were available to attach to the MC-LR on the sensor surface, resulting in a lower electron-transfer resistance. In the Nyquist plots (**Figure 10**(c)), it was obvious that increasing MC-LR concentration caused the decrease of electron transfer impedance on the Anti-MC-LR/MC-LR/Cysteamine/SPCE biosensor. Therefore, the peak values (Z_{max}) of the Nyquist plot reflects the concentration of antibodies bound on the surface of the electrode in a concentration-dependent manner. These results suggested that the correlation between Z_{max} and MC-LR concentrations can be determined by measuring standard serial dilutions of MC-LR mixed with a constant antibody concentration. **Figure 10**(d) shows the calibration curve, which display the linearity on MC-LR. The correlation is Z_{max} = -0.68 × log ([MC-LR]) + 4.23 with R^2 = 0.95 for the developed biosensor, where Z_{max} is the peak value observed on the Nyquist plot and [MC-LR] is the concentration of MC-LR (ng L^{-1}). The LOD was calculated to be 0.69 ng L^{-1}, accomplishing the detection of a much lower concentration than the limit for MC-LR in drinking water guideline of 1 μg L^{-1} according to the WHO and 8 μg L^{-1} for recreational use recommended by the USEPA [7].

Reproducibility was investigated by multiple measurements of the certain MC-LR concentrations and plotting the average and standard deviations (**Figure 10**(d)). For the developed MC-LR detection biosensor, MC-LR concentrations of 10^{-4}, 10^{-5}, and $10^{-5.5}$ g L^{-1} had RSD values 1-19%. These results indicated acceptable reproducibility and feasibility of the biosensors. Another reproducibility test of the Anti-MC-LR/MC-LR/Cysteamine/SPCE biosensor was

conducted using newly prepared solutions. The analysis of the sample with MC-LR concentration of 10^{-5} g L^{-1} showed an error of approximately 3.8% (**Figure 10**(d)).

The MC-LR detection concentration range could be shifted to detect higher or lower concentration by changing the concentration of the antibody. Other solutions to adjust the MC-LR detection ranges can be to increase the size of the working electrode or add nanoparticles to increase the available area which the MC-LR can be present on the surface, allowing for more bonding sites for the antibody allowing for a lower detection limit. However, the current working range seems to be appropriate with regards to regulations and typical MC-LR concentrations found in water bodies experiencing HABs.

4.3.2. Selectivity and Interference

To evaluate the selectivity of the developed Anti-MC-LR/MC-LR/Cysteamine/SPCE biosensor against other MCs, samples with equal concentrations of 10^{-5} g L^{-1} of MC-LR and 10^{-5} g L^{-1} of other common MCs (i.e., MC-YR and MC-RR) were tested under the same condition. As shown in **Figure 11**(a), the electrochemical response for MC-LR including the other MC toxins corresponds to the signal created by the MC-LR sample. The mixed sample (i.e., MC-LR+MC-LR+MC-RR) also showed no significant changes in electron-transfer resistance for MC-LR of 10^{-5} g L^{-1}. The results had an error range of 0.1 – 6.0% and RSD range of 10 - 16%, suggesting high selectivity of the biosensor toward MC-LR.

Finally, specific interference of various possible coexisting ions on the MC-LR detection using the biosensor was also investigated. The tested samples included 10^{-5} g L^{-1} of MC-LR and

82.4 g L^{-1} NaCl, 143 g L^{-1} MgCl$_2$, 3.93 g L^{-1} CuSO$_4$, and/or 53.7 g L^{-1} CaSO$_4$, which are commonly found in natural surface water. The electrochemical signals of the Anti-MC-LR/MC-LR/Cysteamine/SPCE biosensor towards the different ions is shown in **Figure 11**(b). The error ranged was 1.6 - 17.7% and the RSD range was 3 - 10%, where the most interference was observed for the mixed solution containing all the ions, probably due to increased ion strength. However, the interfering test results still show that the biosensor has an acceptable performance for the measurement of MC-LR against the interference of certain ions in water.
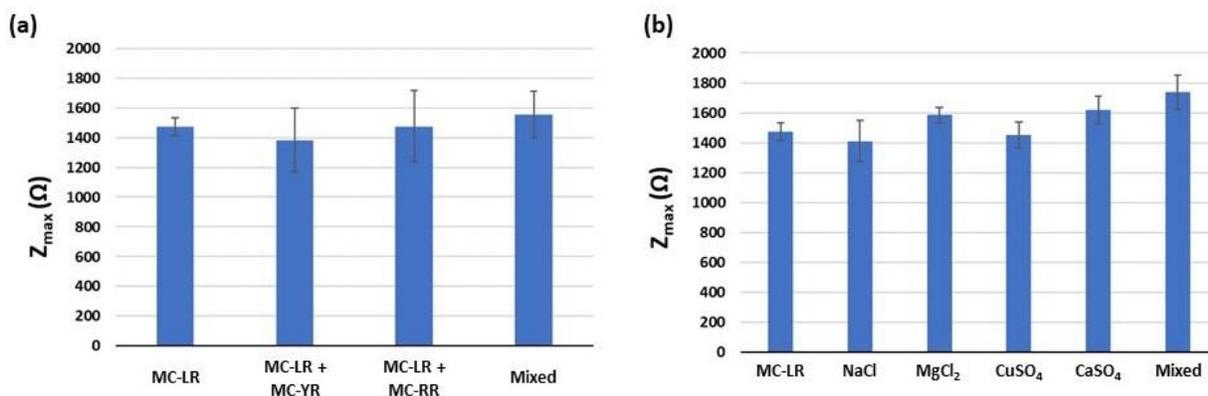
Figure 11. *(a) Selectivity toward other MCs and (b) possible interfering ions effect on the developed biosensor response.*

4.3.3. Sensor Lifetime

The several biosensors were prepared and tested to determine the shelf-life after development. It was previously reported that gold electrodes for MC-LR detection show good functionality for up the 12 weeks [50]. The carbon-based MC-LR detection biosensors developed in this study were stored in the refrigerator (~4 ⁰C) for 5 and 12 weeks and then tested using the

known sample with an MC-LR concentration of 10^{-6} g L^{-1}. The results of the test showed an average error of 16% for 5 weeks and 23% for 12 weeks where the measured resistance of the old sensors was slightly lower than the resistance measured by the sensors tested on the same day as functionalization. However, these results indicate that the sensor has acceptable stability and functionality up to 12 weeks.

4.4. Applications for Surface Water Samples

To evaluate sensor performance in real surface water samples, the Anti-MC-LR/MC-LR/Cysteamine/SPCE biosensor was investigated for the determination of MC-LR extracted from cyanobacteria in the water experiencing HABs in South Korea. After the cyanobacteria was lysed with sonication and the sample was filtered with a 0.22 μm membrane filter, the MC-LR concentration was determined to be 0.43 μg L^{-1} using ELISA. As the MC-LR concentration from the natural water sample was relatively low to test the biosensor performance, we spiked known MC-LR concentrations to create MC-LR concentrations of 10^{-5}, 10^{-6}, and 10^{-7} g L^{-1} to test the biosensor performance. The MC-LR concentrations in the test samples were also validated using ELISA. From **Figure 12**, the Anti-MC-LR/MC-LR/Cysteamine/SPCE biosensor showed good sensitivity toward MC-LR with well-defined Z_{max} values with different MC-LR concentrations in natural surface water. Similar results of MC-LR detection was observed in the surface water samples with the developed biosensor and ELISA, suggesting minimal impact on possible interference of ions (e.g., K^+, Na^+, Cu^{2+}, Cl^-) during MC-LR detection using the Anti-MC-LR/MC-LR/Cysteamine/SPCE biosensor. Based on the constructed calibration curve, the natural water

sample has an MC-LR concentration of 0.46 µg L^{-1} which is a difference of 6.5% compared to the ELISA test result with and RSD value of 0.64%. Overall, the Anti-MC-LR/MC-LR/Cysteamine/SPCE biosensor showed good applicability to surface water samples. However, as shown in **Figure 12**, it is recommended that a site-specific calibration curve be constructed periodically to ensure representativeness of the sensor performance in the water body.
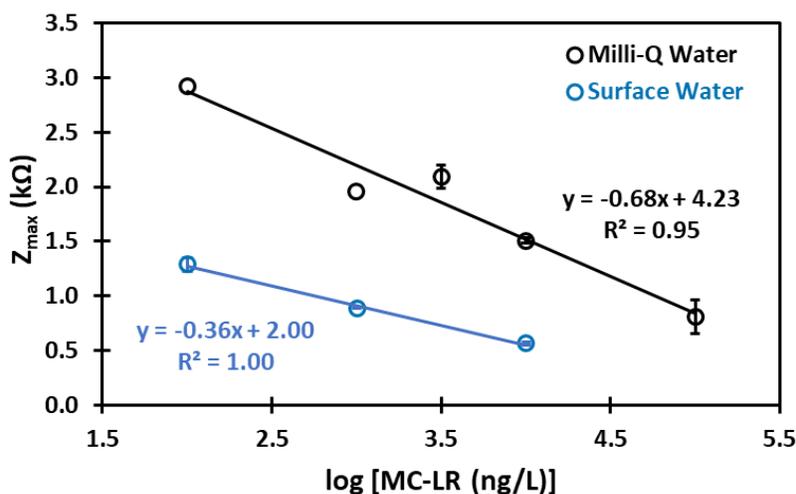
Figure 12. *Standard curve established for Milli-Q water base and surface water base.*

The MC-LR detection performance of the Anti-MC-LR/MC-LR/Cysteamine/SPCE biosensor was comparable with other sensors which are listed in **Table 2**. There are two methods for MC-LR detection: direct [40, 41, 43, 46] and indirect [24, 49-51]. The direct method uses an antibody bound to the surface to directly measure the amount of MC-LR in the water sample. On the other hand, the indirect method uses MC-LR immobilized onto the surface of the electrode and mixes a known concentration of antibody in the sample and then measures the amount the antibody which binds to the MC-LR on the surface of the electrode. Previous studies [37, 38] have demonstrated the efficiency of both antibody-coated surfaces and an immobilized MC-LR

molecule coating for the detection of MC-LR in water, however, the indirect method is more commonly studied as it provides a lower detection limit [21, 24, 39, 42, 45, 50].Previous studies report detection limits as low as 0.57 ng L^{-1} for gold surface electrodes [21, 22, 24, 39, 42, 45, 47, 48, 50, 52]. In this study, we also achieved the comparable LOD of 0.69 ng L^{-1}. While most biosensors were based on gold electrode, often with complicated procedures, the developed the Anti-MC-LR/MC-LR/Cysteamine/SPCE biosensor represents a cost-effective and simple measurements of MC-LR in water with low LOD.

CHAPTER 5: CONCLUSION AND RECOMMENDATIONS

In this study, an Anti-MC-LR/MC-LR/Cysteamine/SPCE biosensor has been successfully fabricated and applied for detecting MC-LR in real surface water samples using EIS. The proposed method was able to detect MC-LR with good sensitivity in complicated surface water sample and has the advantages of the low-cost electrode with reliable performances. The working range and LOD of the Anti-MC-LR/MC-LR/Cysteamine/SPCE biosensor was 10^{-7} to 10^{-4} g L^{-1} and 0.69 ng L^{-1}, respectively. Consecutive measurements of various MC-LR samples were conducted and standard deviation ranged between 0.007 and 0.051, and an analysis was conducted with all new solutions resulting in an error of only 3.8%, showing good reproducibility. The lifetime of the biosensor when stored at 4 ºC resulting in an acceptable stability and functionality up to 12 weeks. Based on the surface water curve, a natural water sample containing 0.43 μg L^{-1} of MC-LR tested with the Anti-MC-LR/MC-LR/Cysteamine/SPCE biosensor and compared to ELISA test results had a different of 6.5% and RSD value of 0.64%. This suggests that the Anti-MC-LR/MC-LR/Cysteamine/SPCE biosensor can be used to detect MC-LR in real-world application. Results of the selectivity tested had an error range of 0.1-6% and RSD range of 10-16%, suggesting high selectivity of the biosensor. Results of the interference test had an error ranged of 1.6-17.7% and the RSD range of 3-10%, showing that the biosensor has an acceptable to good resistance against the interference of certain ions in solution. Therefore, the developed biosensor represents an easily operational, low-cost, and quick method for the determination of cyanotoxins.

Recommendations for future progression include analyzing a larger MC-LR concentration range and testing other possible interfering factors, such as pH and conductivity (e.g., ion strength). The current method of measuring EIS is with the use of PalmSens 4, this system is portable,

however expensive. Therefore, another future work would be the development of a cost effect portable method of measuring EIS, such as with the use of a microcontroller system [24] (e.g. Arduino). With the developed microcontroller system, the biosensor could then be implemented as a real-world cost-effective analysis method. Improvements to the biosensor could be the addition of a blocking layer to the fabrication process, such as bovine serum albumin (BSA). BSA is typically used as a blocking agent to saturate the excess sites on the SAM layer to prevent non-specific binding [71]. This could be used decrease the potential of unwanted ions sticking to the surface of the electrode during the sample analysis step. Also, the fabrication of a direct detection method sensor, as discussed in the literature review (Section 2.3.1), could be beneficial for a potentially more rapid and simplistic detection process.

APPENDIX A: PRELIMINARY TEST RESULTS USING SCREEN-PRINTED GOLD

ELECTRODE (SPGE)

A.1. Cysteamine/MC-LR/anti-MC-LR-SPGE biosensor Electrochemical characterization

In our first test, we initially fabricated the MC-LR detection biosensors using a screen-printed gold electrode (SPGE) to demonstrate the technical feasibility of electrochemical MC-LR detection. The surface functionalization was conducted with the same procedures as described in section 3.2.

The electrode functionalization with Anti-MC-LR/MC-LR/Cysteamine/SPGE biosensor was evaluated through the redox behavior of the cysteamine monolayer by CV recorded using 0.005 M $[Fe(CN)_6]^{3-/4-}$ via different substrate layers (**Figure 13**(a)). The highest redox peak current (14 µA) was observed with the bare gold electrode do of the absence of the SAM nanolayer on the working electrode. The second highest peak (10 µA) SAM layer, which was attributed to the improvement in electron transport due to an electrostatic attraction between the positively charged cysteamine monolayer and the negatively charged redox probe solution [70]. A slight decrease to 8 µA was observed with the addition of the MC-LR, suggesting that binding of the MC-LR acts as a charge insulator from the probe solution and in turn decreases the current response.

The Nyquist plots shown in **Figure 13**(b) were fitted with equivalent circuit models using EIS operation parameters including 0.005 mV and 0.01 V for the DC and AC and a frequency range of 0.1 Hz – 50 kHz. The bare gold electrode showed the lower peak values of 30.6 kΩ. The formation of the cysteamine SAM on the electrode generated a barrier to the interfacial electron-transfer [72] which led to an increase in the peak value to 344 kΩ. The MC-LR resulted in an increase in the Nyquist plot peak value to 1,094 kΩ, demonstrating the successful binding of MC-LR onto SAM layer, as demonstrated by the result of the CV. The EIS detection of MC-LR is based on an inhibition type-immunoassay: the binding of the antibodies to the MC-LR

immobilized onto the electrodes surface is limited by the MC-LR present in the sample that was allowed to react with the antibody before exposure to the sensor. The MC-LR detection concentration range could be shifted to detect higher or lower concentration by changing the concentration of the antibody. Other solutions can be to increase the size of the working electrode or add nanoparticles to increase the available area which the MC-LR can be present on the surface, allowing for more bonding sites for the antibody allowing for a lower detection limit.
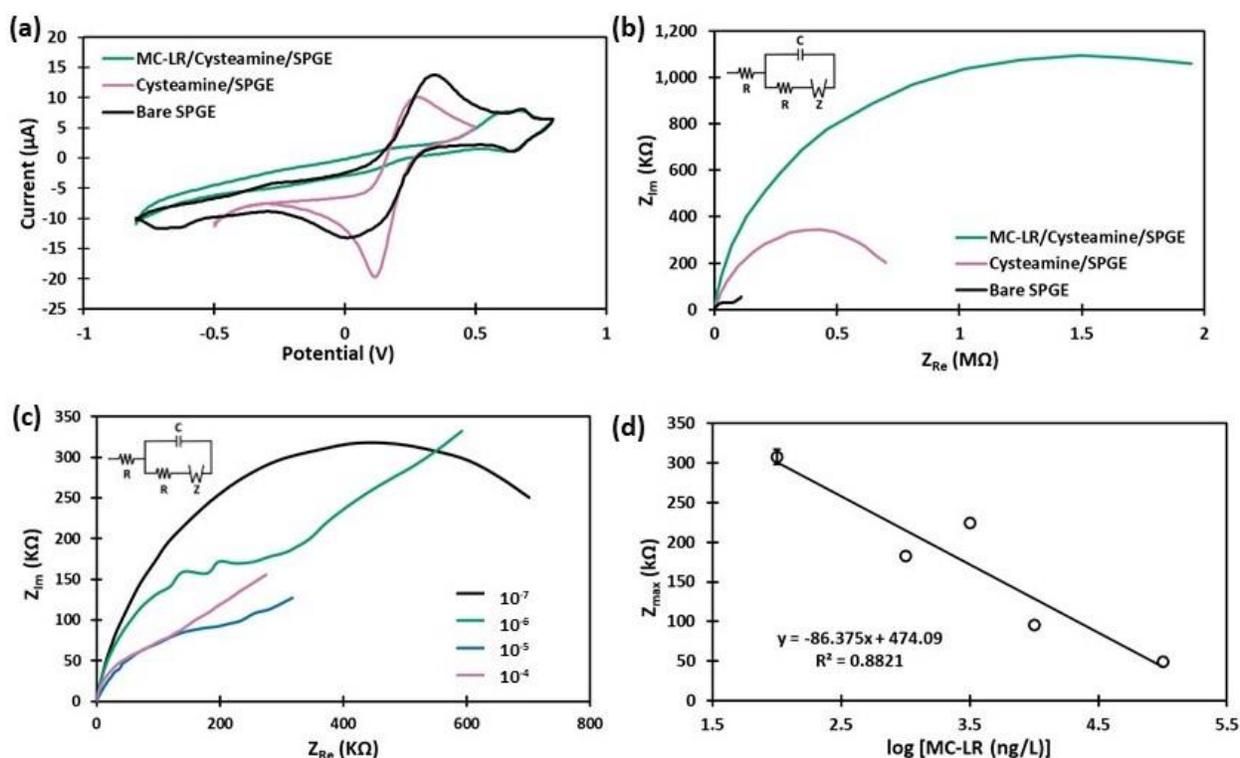

Figure 13. *Anti-MC-LR/MC-LR/Cysteamine/SPGE biosensor: (a) CV curves, (b) Nyquist plots (c) Nyquist plots with different MC-LR concentrations, and (d) Standardized curve for varying MC-LR test samples.*

A.2 Analytical performance of Cysteamine/MC-LR/anti-MC-LR-SPGE biosensor

EIS measurements were further carried out to characterize the binding between immobilized MC-LR and the antibody. In order to develop a sensitive electrochemical method for MC-LR detection, EIS measurements was used to examine the effect of the concentration of MC-LR on the electrochemical signal in the redox probe solution (0.005 M $[Fe(CN)_6]^{3-/4-}$ in PBS) at Anti-MC-LR/MC-LR/Cysteamine/SPGE biosensor (**Figure 13** (c)). In the Nyquist plot, it was obvious that increasing MC-LR concentration caused the decrease of electron transfer impedance on the Anti-MC-LR/MC-LR/Cysteamine/SPGE biosensor. Therefore, the peak values (Z_{max}) of the Nyquist plot reflects the concentration of antibodies bound on the surface of the electrode in a concentration-dependent manner. These results suggested that the correlation between Z_{max} and MC-LR concentrations can be determined by measuring standard serial dilutions of MC-LR mixed with a constant antibody concentration. **Figure 13** (d) shows the calibration curve, which display the linearity on MC-LR. The correlation is $Z_{max} = -86.375 \times \log([MC-LR]) + 474.09$, ($R^2 = 0.88$) for the Anti-MC-LR/MC-LR/Cysteamine/SPGE biosensor, respectively, where Z_{max} is the peak value observed on the Nyquist plot and [MC-LR] is the concentration of MC-LR (ng L^{-1}). The carbon-based Anti-MC-LR/MC-LR/Cysteamine/SPCE biosensor showed a slightly more consistent trend than the gold based Anti-MC-LR/MC-LR/Cysteamine/SPGE. The LOD was 23 ng L^{-1} for the Anti-MC-LR/MC-LR/Cysteamine/SPGE, accomplishing the detection of a much lower concentration than the limit for MC-LR in drinking water guideline of 1 μg L^{-1} according to the World Health Organization (WHO) and 8 μg L^{-1} for recreational use recommended by the EPA [7].

APPENDIX B: DETAILED PROCEDURES

Solutions:

1. Milli-q water collected

    a. Note: For milli-q water, the bottle was autoclaved before obtaining milli-q water

        and then autoclaved on slow with water.

2. 0.00138 g of cysteamine was added to 1 mL of milli-q water to create 18mM solution

3. 0.00434 g of sulfo-NHS was added to 1 mL of milli-q water to create 20 mM

4. 0.01534 g of EDC was added to 1 mL of milli-q water to create 80 mM

5. 10^{-2} g/L solution of MC-LR

    a. 1 mL of milli-q water added to 100 µg of MC-LR to make 0.1 g/L

    b. 1 µL of solution added to additional 9 µL of milli-q water to make 0.01 g/L

6. 10^{-2} g/L solution of Anti-MC-LR (mAb)

    a. 0.2 mL of milli-q water was added to 200 µg mAb (1 g/L)

    b. 99 µL of milli-q water was added to 1 µL of mAb solution (0.01 g/L)

7. Phosphate Buffer (PB, 0.01 M) solution

    a. 0.11998 g NaH_2PO_4 and 0.14196 g Na_2HPO_4 in 100 mL milli-q water

Cleaning:

1. Electrode is cleaned with acetone in an ultrasound bathing for 90 min

    a. Small amount of acetone poured into sample tube

    b. Sensor is added so that the working electrode is completely submerged

    c. Lid is applied

    d. Tube is placed in large beaker of water and ultrasound

        i. ultrasound set for continuous (no pulse), amplitude = 25%

    ii. Make sure tubes are not touching sides of beaker or probe

2. Sensor was removed from tube using tweezers and placed in a petri dish with Kimwip

3. The sensor was dried with N_2

   Note: If Kimwip paper is not used, the sensor will stick to the petri dish.

4. The working electrode was rinsed with Isopropanol and then milli-q water and put back in the petri dish and dried with N_2 again.

Functionalization:

1. 3 μL of 18mM cysteamine is dropped onto the working electrode

2. Sensor is stored in a dark environment for 4 hours to let dry (put in a box)

3. Electrode is rinsed with milli-q water and dried with N_2

4. MC-LR is activated using equal concentrations of 10^{-2} g/L MC-LR, 20 mM sulfo-NHS, and 80 mM EDC and mixed using centrifuge for 30 min at 500 rpm

5. 1 μL is dropped onto working electrode and stored in fridge overnight

6. Electrode is rinsed with milli-q water and dried with N_2

Testing:

1. Equal concentrations of 10^{-2} g/L mAb, PB, and selected MC-LR concentration are centrifuged for 30 min at 500 rpm.

2. 1 μL of solution is dropped onto the sensor and incubated for 1 hour at room temperature.

3. The sensor is rinsed with PB solution.

4. The sensor is tested in redox probe solution (5 mM $[Fe(CN)_6]^{3-}$ in 10 mM PBS).

  a. 0.164625 g $K_3[Fe(CN)_6)]$ + 1 mL stock PBS (x1) + 99 mL DI water

Measurement Settings:

1. Conduct EIS measurements (Carbon)

    a. t equilibration = 20s

    b. E dc = 0.0005 V

    c. E ac = 0.25 V

    d. N frequency = 55

    e. Max frequency = 100,000 Hz

    f. Min frequency = 0.01 Hz

    g. T Max. OCP = 1 s

    h. Stability criterion = 0

    i. All pretreatment settings = 0

2. CV measurements

    a. All pretreatment = 0

    b. t equilibrium = 8

    c. E begin = -0.5

    d. E vertex 1 = -0.5

    e. E vertex2 = 0.5

    f. E step = 0.01

    g. Scan rate = 0.05

    h. Number scans = 3

APPENDIX C: SUPPLEMENTARY INFORMATION FOR CHAPTER 3

Step 1: In a 50mL graduated polypropylene tube, ~10 mL of acetone is added to completely submerge the working electrode on the sensor.

Step 2: Tubes were placed in a large breaker full of water and sonicated for 90 min using probe type ultrasonic bath.
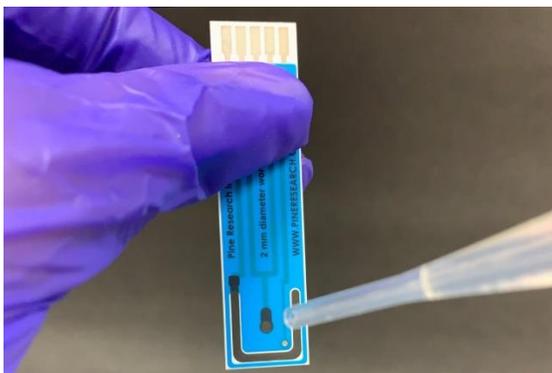
Step3: WE was rinsed with isopropanol and milli-q water
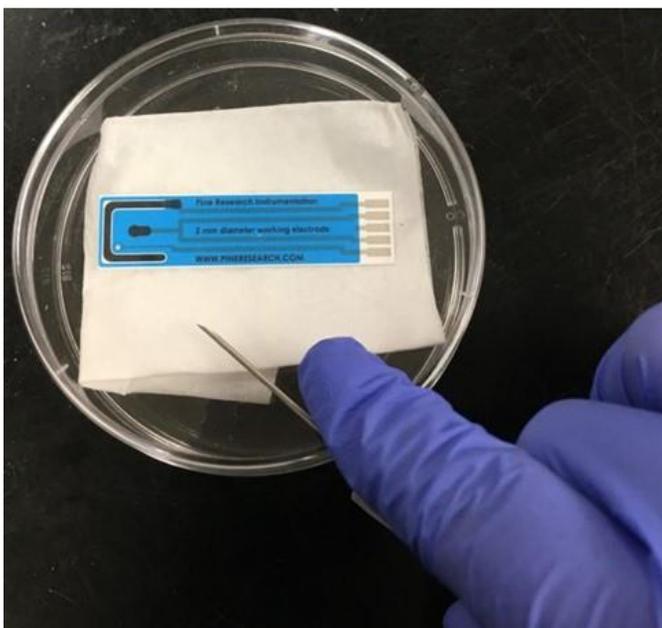
Step 4: WE was dried with N$_2$ gas.
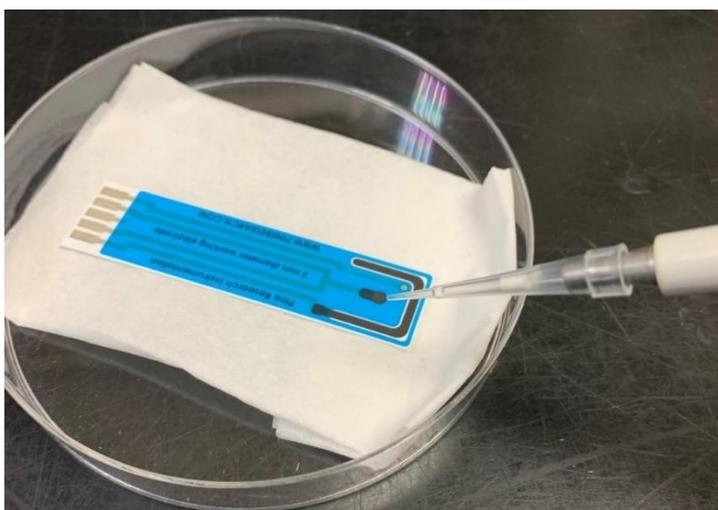
Step 5: 3 µL of 18 mM cysteamine was dropped onto the working electrode.

Step 6: Sensors were placed in a dark and semi-humid environment for 4 hours, for cysteamine to form monolayer.

Step 7: The WE was rinsed with milli-q water and dry with N_2 gas.

Step 8: MC-LR was activated using equal portions of 20 mM sulfo-NHS, 80 mM EDC, and 10^{-2} g/L of MC-LR and spun in the centrifuge at 500 rpm, room temperature for 30 min.

Step 9: The sensors were incubated in the refrigerator overnight to allow the MC-LR to immobilize onto the SAM layer.

Step 10: The WE was rinsed with milli-q water and dry with N_2 gas.

Step 11: Equal amounts of 10^{-2} g/L of anti-MC-LR, PB and sample were mixed in the centrifuge (same as step 8) and 1 μL of sample solution was dropped onto the WE.
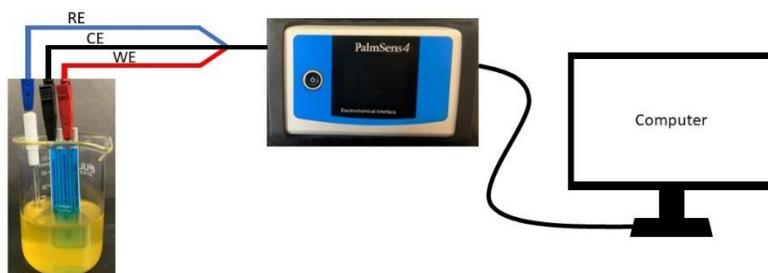
Step 12: The sensor was analyzed using PalmSens.

APPENDIX D: ELISA PROCEDURES

EPA method 546 [13], enzyme-linked immunosorbent assay (ELISA), was used as the accepted accurate standard method to validate the accuracy of the developed biosensor. The Abnova™ Microcystin-LR ELISA Kit was used following the procedures. All materials are removed from the fridge and allowed to warm to room temperature, approximately 2 hours. The wash buffer solution is prepared by diluting the provided buffer solution by 10 times. The desired amount of antibody coated strips was removed from the aluminum pouch, leaving the remaining inside and the pouch was resealed. The wells were rinsed three times with the wash buffer solution, avoiding cross-contamination between the wells. The wells were inverted and tapped on a paper towel to remove any remaining drops. Then 40 μL of the dilution buffer was pipetted into each of the wells being used and then 40 μL of the desired standard or sample was pipetted into the wells. Doubles of each was conducted to reduce errors. The wells were then incubated for 45 minutes at room temperature. Then 20 μL of MC-LR labeled with horseradish (Px-conjugate) was pipetted into each well, this caused the solution to turn a deep blue. The wells are placed on a plate and a shaker was used at 240 rpm for 15 minutes at room temperature. The solution in the wells was dumped into a collection bottle and the wells were rinsed five time with the wash buffer. The wells were again inverted onto a paper towel to remove any remaining liquid. 100 μL of chromogenic substrate (TMB) was added to each of the wells, this solution has a blue tint. The plate was covered with aluminum foil and incubated at room temperature for 20 minutes. The solution was then bright blue. 100 μL of the stop solution was added to each of the wells, the plate was gentle tapped and swirled to ensure complete mixing. The absorbance of the wells was conducted at 450 nm using a microplate reader. A standard curve of the absorbance was developed using the provided stock solutions, concentrations of $0 - 2.5$ μg L^{-1}.

REFERENCES

[1]   L. Backer, D. Manassaram-Baptiste, R. LePrell, and B. Bolton, "Cyanobacteria and algae blooms: review of health and environmental data from the Harmful Algal Bloom-Related Illness Surveillance System (HABISS) 2007–2011," *Toxins,* vol. 7, no. 4, pp. 1048-1064, 2015.

[2]   K. Dyson and D. D. Huppert, "Regional economic impacts of razor clam beach closures due to harmful algal blooms (HABs) on the Pacific coast of Washington," *Harmful Algae,* vol. 9, no. 3, pp. 264-271, 2010 2010, doi: 10.1016/j.hal.2009.11.003.

[3]   E. P. Preece, F. Joan Hardy, B. C. Moore, and M. Bryan, "A review of microcystin detections in Estuarine and Marine waters: Environmental implications and human health risk," *Harmful Algae,* vol. 61, pp. 31-45, 2017 2017, doi: 10.1016/j.hal.2016.11.006.

[4]   D. P. Lesley V. D'Anglada, "EPA's Drinking Water Health Advisories and Recreational Criteria for Cyanotoxins," *US Environmental Protection Agency,* vol. Office of Water/Office of Science and Technology, no. EPA's Region 5 HABs Workshop April 27, 2016 2016. [Online]. Available: https://www.epa.gov/sites/production/files/2016-05/documents/region5-dw-health-advisories.pdf.

[5]   T. Arman and J. D. Clarke, "Microcystin Toxicokinetics, Molecular Toxicology, and Pathophysiology in Preclinical Rodent Models and Humans," *Toxins,* vol. 13, no. 8, p. 537, 2021.

[6]   V. Poretti *et al.*, "2020 Cyanobacterial Harmful Algal Bloom (HAB) Freshwater Recreational Response Strategy," *NJ Department of Environmental Protection,* 2020.

[7]   USEPA, "Recommended human health recreational ambient water quality criteria or swimming advisories for microcystins and cylindrospermopsin (EPA 822-R-19-001)," 2019.

[8]   U. EPA, "Monitoring and Responding to Cyanobacteria and Cyanotoxins in Recreational Waters," 2021. [Online]. Available: https://www.epa.gov/cyanohabs/monitoring-and-responding-cyanobacteria-and-cyanotoxins-recreational-waters.

[9]   J. Park, K. T. Kim, and W. H. Lee, "Recent advances in information and communications technology (ICT) and sensor technology for monitoring water quality," *Water,* vol. 12, no. 2, p. 510, 2020.

[10]   USGS, "Satellite Imagery Used to Measure Algal Bloom Frequency—Steps Toward Understanding Exposure Risk," 2017. [Online]. Available: https://www.usgs.gov/programs/environmental-health-program/science/satellite-imagery-used-measure-algal-bloom-frequency.

[11]   (2015). *METHOD 544. DETERMINATION OF MICROCYSTINS AND NODULARIN IN DRINKING WATER BY SOLID PHASE EXTRACTION AND LIQUID CHROMATOGRAPHY/TANDEM MASS SPECTROMETRY (LC/MS/MS)*

[12]   U. S. EPA, "Method 8315A (SW-846): Determination of Carbonyl Compounds by High Performance Liquid Chromatography (HPLC)," 1996.

[13]   (2016). *Method 546: Determination of Total Microcystins and Nodularins in Drinking Water and Ambient Water by Adda Enzyme-Linked Immunosorbent Assay*.

[14]   M. Pilevar, K. T. Kim, and W. H. Lee, "Recent advances in biosensors for detecting viruses in water and wastewater," *Journal of Hazardous Materials,* vol. 410, p. 124656, 2021.

[15]   S. Alipoori *et al.*, "Polymer-Based Devices and Remediation Strategies for Emerging Contaminants in Water," *ACS Applied Polymer Materials,* vol. 3, no. 2, pp. 549-577, 2021/02/12 2021, doi: 10.1021/acsapm.0c01171.

[16]   S. Menon, M. R. Mathew, S. Sam, K. Keerthi, and K. G. Kumar, "Recent advances and challenges in electrochemical biosensors for emerging and re-emerging infectious diseases," *Journal of Electroanalytical Chemistry,* p. 114596, 2020.

[17]   S. Nagata *et al.*, "Novel monoclonal antibodies against microcystin and their protective activity for hepatotoxicity," vol. 3, no. 2, pp. 78-86, 1995.

[18]   O. Adamovský, L. Bláhová, J. Kohoutek, M. Oravec, and L. J. B.-V. V. Bláha, "Comparison of antibodies commonly used in ELISA for microcystin analyses in natural waters," vol. 47, no. 3, pp. 5-11, 2011.

[19]   J.-W. Sheng, M. He, and H.-C. Shi, "A highly specific immunoassay for microcystin-LR detection based on a monoclonal antibody," *Analytica Chimica Acta,* vol. 603, no. 1, pp. 111-118, 2007/11/05/ 2007, doi: https://doi.org/10.1016/j.aca.2007.09.029.

[20]   M. Campàs, J.-L. J. B. Marty, and Bioelectronics, "Highly sensitive amperometric immunosensors for microcystin detection in algae," vol. 22, no. 6, pp. 1034-1040, 2007.

[21]   L. Hou *et al.*, "An ultrasensitive competitive immunosensor for impedimetric detection of microcystin-LR via antibody-conjugated enzymatic biocatalytic precipitation," *Sensors and Actuators B: Chemical,* vol. 233, pp. 63-70, 2016/10/05/ 2016, doi: https://doi.org/10.1016/j.snb.2016.04.034.

[22]   J. Zhang, Y. Sun, H. Dong, X. Zhang, W. Wang, and Z. Chen, "An electrochemical non-enzymatic immunosensor for ultrasensitive detection of microcystin-LR using carbon nanofibers as the matrix," *Sensors and Actuators B: Chemical,* vol. 233, pp. 624-632, 2016/10/05/ 2016, doi: https://doi.org/10.1016/j.snb.2016.04.145.

[23]   M. P. Bilibana *et al.*, "Electrochemical Aptatoxisensor Responses on Nanocomposites Containing Electro-Deposited Silver Nanoparticles on Poly(Propyleneimine) Dendrimer for the Detection of Microcystin-LR in Freshwater," *Sensors,* vol. 16, no. 11, 2016, doi: 10.3390/s16111901.

[24]   T. Guan *et al.*, "Point-of-need detection of microcystin-LR using a smartphone-controlled electrochemical analyzer," *Sensors and Actuators B: Chemical,* vol. 294, pp. 132-140, 2019.

[25]   A. Zeck, A. Eikenberg, M. G. Weller, and R. J. A. C. A. Niessner, "Highly sensitive immunoassay based on a monoclonal antibody specific for [4-arginine] microcystins," vol. 441, no. 1, pp. 1-13, 2001.

[26]   W. C. W. Centre, "How to analyze cyanotoxins using the Microcystin-LR equivalents ELISA method," ed, 2016.

[27]   USEPA, "Water treatment optimization for cyanotoxins (EPA 810-B-16-007)," 2016.

[28]   S. Herranz, M. Bocková, M. D. Marazuela, J. Homola, and M. C. Moreno-Bondi, "An SPR biosensor for the detection of microcystins in drinking water," *Analytical and bioanalytical chemistry,* vol. 398, no. 6, pp. 2625-2634, 2010.

[29]   H. Chen, X. Wang, S. Zhan, Z. Luo, and H. Zhou, "A miniature surface plasmon resonance bioanalytical system for field detection of microcystin-Lr in surface water," *Instrumentation Science & Technology,* vol. 39, no. 5, pp. 462-474, 2011.

[30]   P. Katie Thoren, "The Role of Surface Plasmon Resonance in Clinical Laboratories," *AACC Clinical Laboratoey News,* 2019.

[31]   L. Liu *et al.*, "An array fluorescent biosensor based on planar waveguide for multi-analyte determination in water samples," *Sensors and Actuators B: Chemical,* vol. 240, pp. 107-113, 2017/03/01/ 2017, doi: https://doi.org/10.1016/j.snb.2016.08.118.

[32]   L. Liu, X. Zhou, J. S. Wilkinson, P. Hua, B. Song, and H. Shi, "Integrated optical waveguide-based fluorescent immunosensor for fast and sensitive detection of microcystin-LR in lakes: Optimization and Analysis," *Scientific reports,* vol. 7, no. 1, pp. 1-9, 2017.

[33]   S. Herranz, M. D. Marazuela, and M. C. Moreno-Bondi, "Automated portable array biosensor for multisample microcystin analysis in freshwater samples," *Biosensors and Bioelectronics,* vol. 33, no. 1, pp. 50-55, 2012/03/15/ 2012, doi: https://doi.org/10.1016/j.bios.2011.12.016.

[34]   C. Murphy *et al.*, "Detection of the cyanobacterial toxin, microcystin-LR, using a novel recombinant antibody-based optical-planar waveguide platform," *Biosensors and Bioelectronics,* vol. 67, pp. 708-714, 2015/05/15/ 2015, doi: https://doi.org/10.1016/j.bios.2014.10.039.

[35]   Z. Wang, J. Yu, R. Gui, H. Jin, and Y. Xia, "Carbon nanomaterials-based electrochemical aptasensors," *Biosensors and Bioelectronics,* vol. 79, pp. 136-149, 2016/05/15/ 2016, doi: https://doi.org/10.1016/j.bios.2015.11.093.

[36]   S. G. Meirinho, L. G. Dias, A. M. Peres, and L. R. Rodrigues, "Voltammetric aptasensors for protein disease biomarkers detection: A review," *Biotechnology Advances,* vol. 34, no. 5, pp. 941-953, 2016/09/01/ 2016, doi: https://doi.org/10.1016/j.biotechadv.2016.05.006.

[37]   C. Han *et al.*, "A multiwalled-carbon-nanotube-based biosensor for monitoring microcystin-LR in sources of drinking water supplies," vol. 23, no. 14, pp. 1807-1816, 2013.

[38]   J. Zhang, J. Lei, C. Xu, L. Ding, and H. J. A. c. Ju, "Carbon nanohorn sensitized electrochemical immunosensor for rapid detection of microcystin-LR," vol. 82, no. 3, pp. 1117-1122, 2010.

[39]   P. Tong, S. Tang, Y. He, Y. Shao, L. Zhang, and G. Chen, "Label-free immunosensing of microcystin-LR using a gold electrode modified with gold nanoparticles," *Microchimica Acta,* vol. 173, no. 3-4, pp. 299-305, 2011.

[40]   X. Sun, H. Shi, H. Wang, L. Xiao, and L. Li, "A Simple, Highly Sensitive, and Label-Free Impedimetric Immunosensor for Detection of Microcystin-LR in Water," *Analytical Letters,* vol. 43, no. 4, pp. 533-544, 2010/02/17 2010, doi: 10.1080/00032710903406912.

[41]   Q. Wei *et al.*, "Nanoporous PtRu Alloy Enhanced Nonenzymatic Immunosensor for Ultrasensitive Detection of Microcystin-LR," *Advanced Functional Materials,* vol. 21, no. 21, pp. 4193-4198, 2011.

[42]   Y. Zhang *et al.*, "A molybdenum disulfide/gold nanorod composite-based electrochemical immunosensor for sensitive and quantitative detection of microcystin-LR in environmental samples," *Sensors and Actuators B: Chemical,* vol. 244, pp. 606-615, 2017.

[43]   K. Zhang *et al.*, "A competitive microcystin-LR immunosensor based on Au NPs@metal-organic framework (MIL-101)," *Chinese Chemical Letters,* vol. 30, no. 3, pp. 664-667, 2019/03/01/ 2019, doi: https://doi.org/10.1016/j.cclet.2018.10.021.

[44] M. Campàs and J.-L. Marty, "Highly sensitive amperometric immunosensors for microcystin detection in algae," *Biosensors and Bioelectronics,* vol. 22, no. 6, pp. 1034-1040, 2007/01/15/ 2007, doi: https://doi.org/10.1016/j.bios.2006.04.025.

[45] L. Talamini, N. Zanato, E. Zapp, D. Brondani, and I. C. Vieira, "Direct Electrochemical Nano-immunosensor for Microcystin-LR in Seawater," *Electroanalysis,* vol. 30, no. 5, pp. 819-827, 2018.

[46] P. Pang *et al.*, "Ultrasensitive enzyme-free electrochemical immunosensor for microcystin-LR using molybdenum disulfide/gold nanoclusters nanocomposites as platform and Au@Pt core-shell nanoparticles as signal enhancer," *Sensors and Actuators B: Chemical,* vol. 266, pp. 400-407, 2018/08/01/ 2018, doi: https://doi.org/10.1016/j.snb.2018.03.154.

[47] Z. Lin *et al.*, "Determination of microcystin-LR in water by a label-free aptamer based electrochemical impedance biosensor," *Talanta,* vol. 103, pp. 371-374, 2013.

[48] K. Zhang, H. Ma, P. Yan, W. Tong, X. Huang, and D. D. Chen, "Electrochemical detection of microcystin-LR based on its deleterious effect on DNA," *Talanta,* vol. 185, pp. 405-410, 2018.

[49] J. Zhang, J. Lei, C. Xu, L. Ding, and H. Ju, "Carbon Nanohorn Sensitized Electrochemical Immunosensor for Rapid Detection of Microcystin-LR," *Analytical Chemistry,* vol. 82, no. 3, pp. 1117-1122, 2010/02/01 2010, doi: 10.1021/ac902914r.

[50] M. B. dos Santos *et al.*, "Portable sensing system based on electrochemical impedance spectroscopy for the simultaneous quantification of free and total microcystin-LR in freshwaters," *Biosensors and Bioelectronics,* vol. 142, p. 111550, 2019.

[51] C. Gan, Z. Sun, L. Ling, Z. He, H. Lei, and Y. Liu, "Construction of portable electrochemical immunosensors based on graphene hydrogel@ polydopamine for microcystin-LR detection using multi-mesoporous carbon sphere-enzyme labels," *RSC advances,* vol. 6, no. 57, pp. 51662-51669, 2016.

[52] S. Loyprasert, P. Thavarungkul, P. Asawatreratanakul, B. Wongkittisuksa, C. Limsakul, and P. Kanatharana, "Label-free capacitive immunosensor for microcystin-LR using self-assembled thiourea monolayer incorporated with Ag nanoparticles on gold electrode," *Biosensors and Bioelectronics,* vol. 24, no. 1, pp. 78-86, 2008/09/15/ 2008, doi: https://doi.org/10.1016/j.bios.2008.03.016.

[53] A. Zeck, A. Eikenberg, M. G. Weller, and R. Niessner, "Highly sensitive immunoassay based on a monoclonal antibody specific for [4-arginine]microcystins," *Analytica Chimica Acta,* vol. 441, no. 1, pp. 1-13, 2001/08/16/ 2001, doi: https://doi.org/10.1016/S0003-2670(01)01092-3.

[54] W. H. Lee, D. G. Wahman, and J. G. Pressman, "Amperometric carbon fiber nitrite microsensor for in situ biofilm monitoring," *Sensors and Actuators B: Chemical,* vol. 188, no. 0, pp. 1263-1269, 11// 2013, doi: http://dx.doi.org/10.1016/j.snb.2013.08.058.

[55] X. Wu, L. Hou, X. Lin, and Z. Xie, "Chapter 12 - Application of Novel Nanomaterials for Chemo- and Biosensing of Algal Toxins in Shellfish and Water," in *Novel Nanomaterials for Biomedical, Environmental and Energy Applications*, X. Wang and X. Chen Eds.: Elsevier, 2019, pp. 353-414.

[56] M. Hunt, E. Herron, and L. Green, "Chlorides in Fresh Water," *URI Watershed Watch,* 2012.

[57] A. Elbein. (2017) Lakes are Being A-Salted. *Hakai Magazine*.

[58]   S. Morr, E. Cuartas, B. Alwattar, and J. M. Lane, "How much calcium is in your drinking water? A survey of calcium concentrations in bottled and tap water and their significance for medical treatment and drug administration," (in eng), *HSS J,* vol. 2, no. 2, pp. 130-135, 2006, doi: 10.1007/s11420-006-9000-9.

[59]   (2003). *Drinking Water Advisory: Consumer Acceptability Advice and Health Effects Analysis on Sulfate*. [Online] Available: https://www.epa.gov/sites/default/files/2014-09/documents/support_cc1_sulfate_healtheffects.pdf

[60]   (2008). *Public Health Goal for Copper in Drinking Water*. [Online] Available: https://oehha.ca.gov/media/downloads/water/chemicals/phg/copperphg020808.pdf

[61]   I. S. Kim, G.-H. Nguyen, S.-Y. Kim, J.-W. Lee, and H.-W. Yu, "Evaluation of methods for cyanobacterial cell lysis and toxin (microcystin-LR) extraction using chromatographic and mass spectrometric analyses," *Environmental engineering research,* vol. 14, no. 4, pp. 250-254, 2009.

[62]   A. Abdul Razzaq *et al.*, "High-performance lithium sulfur batteries enabled by a synergy between sulfur and carbon nanotubes," *Energy Storage Materials,* vol. 16, pp. 194-202, 2019/01/01/ 2019, doi: https://doi.org/10.1016/j.ensm.2018.05.006.

[63]   F. Ekiz, F. Oğuzkaya, M. Akin, S. Timur, C. Tanyeli, and L. Toppare, "Synthesis and application of poly-SNS-anchored carboxylic acid: a novel functional matrix for biomolecule conjugation," *Journal of Materials Chemistry,* 10.1039/C1JM12048D vol. 21, no. 33, pp. 12337-12343, 2011, doi: 10.1039/C1JM12048D.

[64]   J. B. Gilbert, M. F. Rubner, and R. E. Cohen, "Depth-profiling X-ray photoelectron spectroscopy (XPS) analysis of interlayer diffusion in polyelectrolyte multilayers," *Proceedings of the National Academy of Sciences,* vol. 110, no. 17, pp. 6651-6656, 2013, doi: 10.1073/pnas.1222325110.

[65]   M.-S. Lee, M. Park, H. Y. Kim, and S.-J. Park, "Effects of Microporosity and Surface Chemistry on Separation Performances of N-Containing Pitch-Based Activated Carbons for CO_2/N_2 Binary Mixture," *Scientific Reports,* vol. 6, no. 1, p. 23224, 2016/03/18 2016, doi: 10.1038/srep23224.

[66]   H. Chen *et al.*, "Exploring Chemical, Mechanical, and Electrical Functionalities of Binders for Advanced Energy-Storage Devices," *Chemical Reviews,* vol. 118, no. 18, pp. 8936-8982, 2018/09/26 2018, doi: 10.1021/acs.chemrev.8b00241.

[67]   S. S. Zhang, K. Xu, and T. R. Jow, "Evaluation on a water-based binder for the graphite anode of Li-ion batteries," *Journal of Power Sources,* vol. 138, no. 1, pp. 226-231, 2004/11/15/ 2004, doi: https://doi.org/10.1016/j.jpowsour.2004.05.056.

[68]   K. Yuan *et al.*, "Nitrogen-doped porous carbon/graphene nanosheets derived from two-dimensional conjugated microporous polymer sandwiches with promising capacitive performance," *Materials Chemistry Frontiers,* 10.1039/C6QM00012F vol. 1, no. 2, pp. 278-285, 2017, doi: 10.1039/C6QM00012F.

[69]   D. X. Oh, S. Shin, C. Lim, and D. S. Hwang, "Dopamine-Mediated Sclerotization of Regenerated Chitin in Ionic Liquid," *Materials,* vol. 6, no. 9, pp. 3826-3839, 2013. [Online]. Available: https://www.mdpi.com/1996-1944/6/9/3826.

[70]   R. K. Shervedani, A. Farahbakhsh, and M. Bagherzadeh, "Functionalization of gold cysteamine self-assembled monolayer with ethylenediaminetetraacetic acid as a novel nanosensor," *Analytica Chimica Acta,* vol. 587, no. 2, pp. 254-262, 2007/03/28/ 2007, doi: https://doi.org/10.1016/j.aca.2007.01.053.

[71]   R. Ahirwar, S. Bariar, A. Balakrishnan, and P. Nahar, "BSA blocking in enzyme-linked immunosorbent assays is a non-mandatory step: a perspective study on mechanism of BSA blocking in common ELISA protocols," *RSC advances,* vol. 5, no. 121, pp. 100077-100083, 2015.

[72]   R. K. Shervedani and S. A. Mozaffari, "Preparation and electrochemical characterization of a new nanosensor based on self-assembled monolayer of cysteamine functionalized with phosphate groups," *Surface and Coatings Technology,* vol. 198, no. 1, pp. 123-128, 2005/08/01/ 2005, doi: https://doi.org/10.1016/j.surfcoat.2004.10.025.